Universitetet i Stavanger

FACULTY OF SCIENCE AND TECHNOLOGY

MASTER'S THESIS

Study programme / specialisation: Petroleum engineering / Reservoir Engineering	Spring semester, 2020 Open/~~Restricted~~
Author: Juan Luis Molina Landínez	…… (signature of author)

Faculty supervisor: Assoc. Prof. Anton Shchipanov (UiS)

External supervisor: Gyunay Namazova (Wintershall Dea Norge AS)

Title of master's thesis:

Multi-well Interference Test Analysis

Credits: 30 ECTS

Keywords: Pressure Transient Analysis (PTA) Well interference testing Horizontal wells Reservoir simulation	Number of pages: 81 + supplemental material/other: 0 Stavanger, July 15th/2020 date/year

Title page for Master's Thesis
Faculty of Science and Technology

MULTI-WELL INTERFERENCE TEST ANALYSIS

Summary

Understanding if there is any hydraulic communication, between the wells within a reservoir and a degree of the communication have been a subject of study for a long time. This information becomes crucial when injection schemes are implemented in the oil and gas fields to mobilize the reservoir fluids or support pressure. Interwell tracer tests and interference tests using pressure data are some of the existing methods to determine the hydraulic connectivity between adjacent wells.

The objective of this work is to identify and characterize the reservoir communication between the horizontal producers and production-injection wells using data from one of the oil fields on the Norwegian Continental Shelf. The reservoir in focus is a fault block, limited by sealing faults from sides making well interference of special importance for improving drainage strategy and sweep efficiency. The objective above is achieved by analyzing the pressure transient data collected by permanent downhole gauges in combination with rates.

Conventional interference test interpretations, that use the exponential integral solution approximation, are not used in this study because of the relative short distance between the wells compared to their long horizontal well section, and the interference with the outer reservoir boundaries and/or with the nearby wells that prevented the late pseudo-radial flow from developing at the late time region. Analysis with time-lapse shut-in pressure transients using analytical, and numerical models are carried out instead, to evaluate well interference for the horizontal production wells and the deviated injection well. Additionally, time-lapse Pressure Transient Analysis (PTA) is implemented to evaluate the changes along the time in the well and reservoir parameters.

The PTA using analytical and numerical models showed similar results and both confirmed the well interference between the producers as well as between the producers and the injector. Time-lapse PTA with analytical models has confirmed strong interference between the producers. It was found that interference with wells in production may be similar to wells in shut-in, if these wells significantly depleted pressure in the drainage area before this shut-in.

As a next step, numerical models were applied to address the complex reservoir geometry and the horizontal wells, as analytical models consider the horizontal wells nearby the tested well as vertical wells and the closed system by a rectangular shape. From time-lapse PTA analysis, different behavior in the pressure response in the southern part of the field is obtained before and after water injection. Reservoir heterogeneity is observed in this part of the field having higher kh compared to the northern part of the field, but during injection further increase of kh may be interpreted. Multi-layer model and sensitivity analysis

suggested that the apparent increase in kh after waterflooding is the result of a contribution of an additional layer. This can be explained by activation of some portions within the same main producing layer or an underlaying layer.

The study confirmed capabilities of time-lapse PTA with analytical models to get understanding of interference for long horizontal wells in fault block type of reservoirs. Analytical models are fast in assembling and running, while simplified well and reservoir geometries are capable to capture major pressure behavior in such reservoirs. The well and reservoir parameters from the analytical models were further applied in numerical models giving same quality history match, providing the basis for further study of more complex effects.

Acknowledgements

Thanks to God Almighty for guiding me throughout the project and during my whole life, for providing me with wisdom and giving me the encouragement needed.

I would like to thank my supervisor Gyunay Namazova, Reservoir engineer, at Wintershall Dea Norge AS, for suggesting the topic of my thesis and steering me in the right direction when need it, for her advices and valuable contributions to the fulfilment of the project.

I would like to express my sincere gratitude to my faculty supervisor Associate Professor Anton Shchipanov at UIS and Senior Research Engineer at NORCE. His knowledge, guidance, valuable contributions, and patience are greatly appreciated.

I would also like to acknowledge the contribution of the professionals at Wintershall Dea Norge AS, especially to Alina Afanasyeva, Senior Geologist, who helped me and shared their ideas in related aspects of the thesis.

Access to academic license of Kappa Workstation software from Kappa Engineering is gratefully acknowledged.

I also want to thank my family, my parents, for their support, endlessly love, prayers, and my sister and brother for their continuous encouragement.

Finally, I must express my gratitude to all my friends, inside and outside of Stavanger during my studies, who were part of this journey.

Table of Contents

List of figures

List of tables

1. Introduction

Characterizing the reservoirs is of great importance to manage and produce the oil and gas fields, so that the highest possible recovery can be achieved at the end of the production life. Since the introduction of Pressure Transient Analysis (PTA), it has become possible to characterize the reservoir at a large-scale using pressure and flow rate measurements of the production or injection wells along the time from specific well tests. Nowadays, with the monitoring through Permanent Downhole Gauges (PDG) and the huge amount of data that is collected from it, more analyses can be carried out. When the fields are in the production phase and several wells are simultaneously producing, further information can be obtained apart from the traditional analysis of pressure buildup and drawdown.

In this thesis, a sandstone formation on the Norwegian Continental Shelf is studied. The field is located in a large northeast-southwest trending horst (the northeastern extension of the Trestakk Horst). The main reservoir corresponds to a Middle Jurassic formation and consists of massive sandstone with some thin layers of shale and calcareous nodulus. The thickness variation of the Middle and Lower Jurassic is little over the area. The field is developed with 7 wells, 5 production horizontal wells and 2 deviated water injection wells. According to the structural trap the reservoir can be represented as closed chamber with no internal faults. It is currently produced by water injection to support pressure and the production wells are equipped with gas lift.

In the field, the reservoir pressure declines rapidly and further understanding of the formation through the interference analysis between the production and injection wells could contribute to get more information about the hydraulic connectivity between the production and the injection wells.

1.1 Objectives

The main objective of this project is to characterize the reservoir using Pressure Transient Analysis and the interference analysis between the horizontal production wells and injection wells in the field. To achieve this, analytical and numerical modelling is implemented using the data acquired with permanent downhole gauges.

The objectives can be divided in the following:

- Confirm hydraulic communication between producers.
- Corroborate pressure support from injector to producers.
- Analyze the effect of effective well length with possible changes from time-lapse PTA and compare the results with chemical PLT data.
- Study the effect of producing below bubble point pressure.

- Observe if there are any changes in reservoir parameters and well performance seen from time-lapse PTA.

1.2 Scope

The scope of the thesis can be divided in the following tasks:

- Time-lapse PTA and production wells interference using Saphir software from KAPPA Engineering.
- Multi-well analysis for producers with assembling 2D ‘full-field’ numerical model for upper layer considering single-phase (oil) in Saphir.
- Analysis of injection well with assembling 2D ‘full-field’ model for upper layer.
- Simulations of 3D full-field models including upper and bottom layer including all production and injection wells based on the 2D simulation results.

2. Theoretical Background

Since 1940'ies, when the recording of pressure measurements started, well tests were designed to get information about the reservoir and the well. Nowadays, the approach has been significantly developed, and generally the well tests are performed only in the exploration and appraisal phase, while in the development phase, the introduction of Permanent Downhole Gauges (PDGs) have played a major role to get the pressure data to be interpreted giving understanding of the reservoir behavior.

Pressure Transient Analysis (PTA) is traditionally used to characterize well and reservoir parameters from well tests based on shut-in period (Stewart, 2011). In the modern environment, the installation of PDGs has become commonplace and the pressure and production data are analyzed as a continuous well test. The main motive for running permanent gauges is to allow the capture of buildups resulting from unplanned platform shutdowns (Stewart, 2011) or continuous analysis of flowing periods (Shchipanov et al., 2014).

PTA has experienced multiple advances, where computer power improvements have been a key factor. For some period, the use of derivatives in finding the interpretation method remained as the major breakthrough until the deconvolution, allowing more data for interpretation, other tools also played a major role to develop new interpretation models that allowed to understand and characterize better the reservoir (Gringarten, 2008).

The tests can be classified depending on where the disturbance is made (usually flow rate) and the effect of this is measured (usually pressure). If the flow rate is modified and the pressure is measured in the same well, the test is called "single-well" test. On the other hand, if the flow rate is changed in one well but the pressure is measured in another well, the test is called "multiple-well test". The classification of some common tests is as follows (Kamal, 1983) :

- Single well tests:
  Drawdown test
  Buildup test
  Injectivity test
  Falloff test
  Step rate test

- Multi-well tests:
  Interference test
  Pulse tests

2.1 Interference test

In 1940, the interference tests were introduced by (Jacob, 1940) for water wells and applied 6 years later in the petroleum industry by (Elkins, 1946). Driscoll suggested in 1963 that it was possible to obtain information of the reservoir between the studied wells as average areal transmissibility, storativity and degree of communication (Nurafza et al., 2014).

Interference tests involve several wells. The well where the pulse is generated through a change in the flow rate is called active well and the one where the pressure is measured is called the observation well (Bourdarot, 1998). The active well can produce or inject fluids while measuring the pressure response in the observation well. It is the well response in the observation well that is subject to analysis and since this well is at static conditions the concept of skin and wellbore storage is eliminated. Thus, in the majority of cases, the Line source solution (or the Theis' solution) can be used directly to analyze the observation well pressure response (Houzé & Viturat, 2020).

Within the interference tests, it is possible to find the simple interference test and the multi-well interference test. The first one involves only two wells, a producer or injector as the active and the observation well, while the second one involves one active well and several observation wells (Sabet, 1991) . A schematic of an interference test is shown in Figure 1. Schematic of an example of multi-well interference test.

A time lag exists between the time at which a rate change is made at the active well and the time at which the pressure transient is seen in the observation well (Akin, 2015). The objectives of the interference test are to determine if pressure communication exists between two or more wells in a reservoir and to characterize this hydraulic communication (Chaudhry, 2004). The formation mobility k/μ and the storativity (φ*ct) can be obtained in the reservoir in between (Kuchuk, 2010).

2.2 Interference test analysis in vertical wells

The first technique used to interpret interference test was applying the type curves introduced by Theis in 1935 and matching the pressure response in the log-log scale observed in the observation well after the disturbance in the active well was generated.

The conventional analysis of interference tests is using the exponential integral solution or type curves of Theis in conjunction with the pressure derivative, as shown in Figure 2. Exponential integral solution log-log plot with pressure derivative used in vertical wells. Adapted from (Houzé et al, 2020); the match point in the intersection of the curves for the observation well allows to calculate the permeability thickness product kh/μ and ctφh (Bourdet, 2002). This type curve matching process applied to interference test analysis is easier than using the same approach for single-well testing as only one type curve is used (Chaudhry, 2004). Despite this benefit, in practice, using type-curve for interpretation of interference tests is usually difficult (Bourdet, 2002).

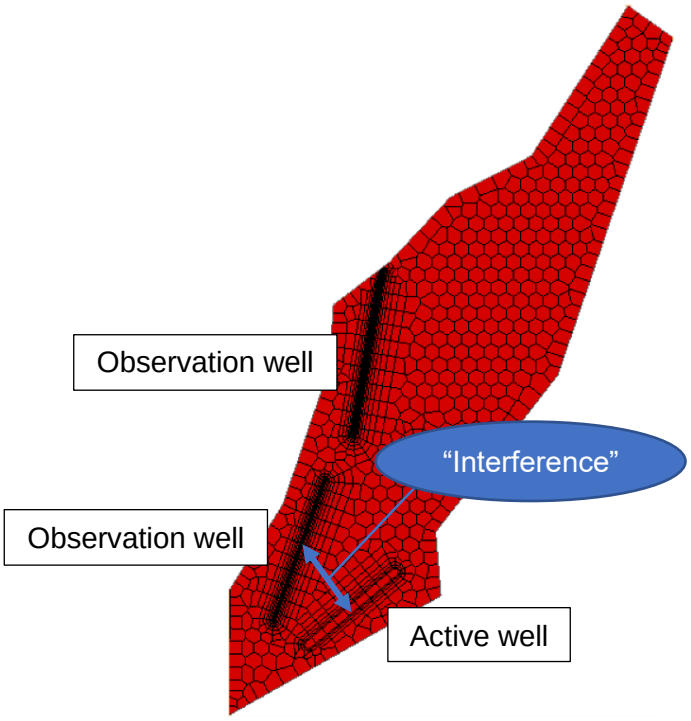

Figure 1. Schematic of an example of multi-well interference test.

The mentioned type curve match or exponential integral solution applies only for homogenous and isotropic reservoirs, neglecting wellbore storage effects and skin damage in both, active and observation well. Later, Ramey (1975) studied the impact of anisotropy in homogenous formations. Bourdet (2002) explained the different effects for closed-system, multi-layer, composite and double porosity reservoirs in interference tests.

With respect to the influence of wellbore storage effects, Bourdet (2002) concluded that when these effects are large, and the distance between the wells is short, the match using the type curves is quite uncertain, and even more if radial flow regime is not obtained at the end of the test.

In addition, according to Kuchuk (2010), the multi-well interference test data may give additional information to φct, allowing to verify the reservoir PV and the estimated distances to sealing boundaries.

Moreover, Bourdet (2002) claimed that if interferences are generated and boundary effects expected, using the analytical model requires good knowledge of the locations of the wells in the boundary geometry.

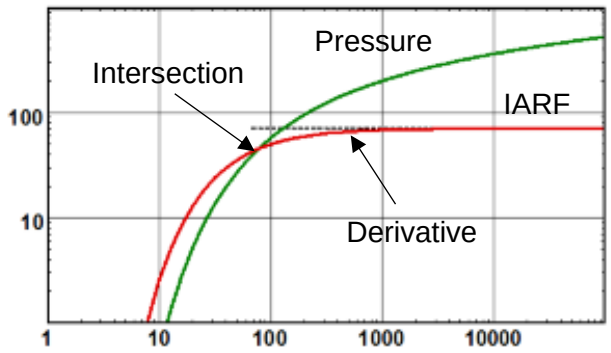

Figure 2. Exponential integral solution log-log plot with pressure derivative used in vertical wells. Adapted from (Houzé et al, 2020)

2.3 Interference test analysis in horizontal wells

The main flow regimes developed in horizontal wells are early-radial, linear flow, and late radial. The early radial is developed if no wellbore storage masked the regime, and the circular flow can be elliptical if there is permeability anisotropy. The linear flow is observed once the transient reaches the upper and lower boundaries and the length of the horizontal well will determine the time required to develop the late radial flow (if its longer it will take more time), this provided that no interference with boundaries or nearby wells are reached by transient. The estimation of kh requires the late radial flow to develop (Houzé & Viturat, 2020). An example of a horizontal well PTA response is shown in the Figure 3. Horizontal well PTA response (Houzé et al, 2020).

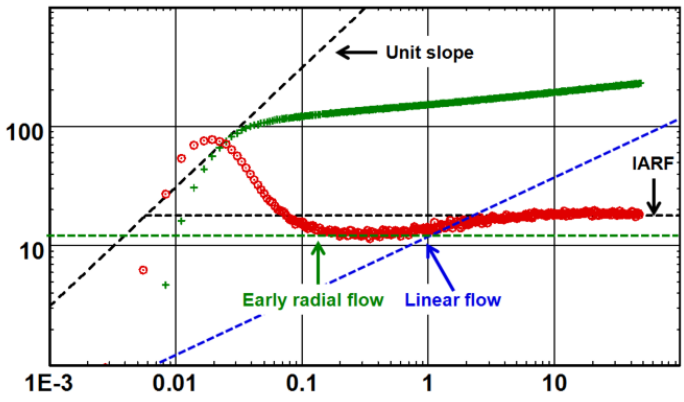

Figure 3. Horizontal well PTA response (Houzé et al, 2020)

Interference tests in horizontal wells were first presented by Malekzadeh & Tiab (1991), developing dimensionless pressure derivative type curves. Al-Khamis et al. (2005) claimed that interpreting interference tests for horizontal wells is challenging due to the considerations in well lengths, orientations, locations, and distances between wells. Additionally, he concluded that treating the observation horizontal well as vertical was required. The decision of replacing the horizontal active well by an equivalent point was recommended if the well spacing was sufficiently large compared to the horizontal well section, and that the location of the point should be estimated instead of selecting the heel or center of the well. By changing the active and observation horizontal wells to vertical wells, the conventional analysis of interference test for vertical wells can be used (M. N. Al-Khamis et al., 2005). The infinite acting radial flow observed in Figure 2. Exponential integral solution log-log plot with pressure derivative used in vertical wells. Adapted from (Houzé et al, 2020) for vertical wells corresponds to the late radial flow for horizontal wells when using the approach for vertical wells.

Furthermore, M. Al-Khamis et al., (2001) presented a semi-analytical model to interpret the interference test of two parallel horizontal wells of equal lengths. Extended later by Awotunde et al., (2008) for the case of unequal lengths. Both models consider anisotropic but homogenous reservoirs.

Permanent well surveillance with PDG is brilliant source of data for studying well interference. Most efficient interference monitoring may be achieved with combined time-lapse analysis of shut-in and flowing data as it was shown for long horizontal wells in Shchipanov et al. (2014). An example of the time-lapse PTA can be observed for an injection well in Figure 4. Time-lapse responses in pressure and derivative for fall-off (left) and injection(right) periods observed in history of a well (Shchipanov, 2014).

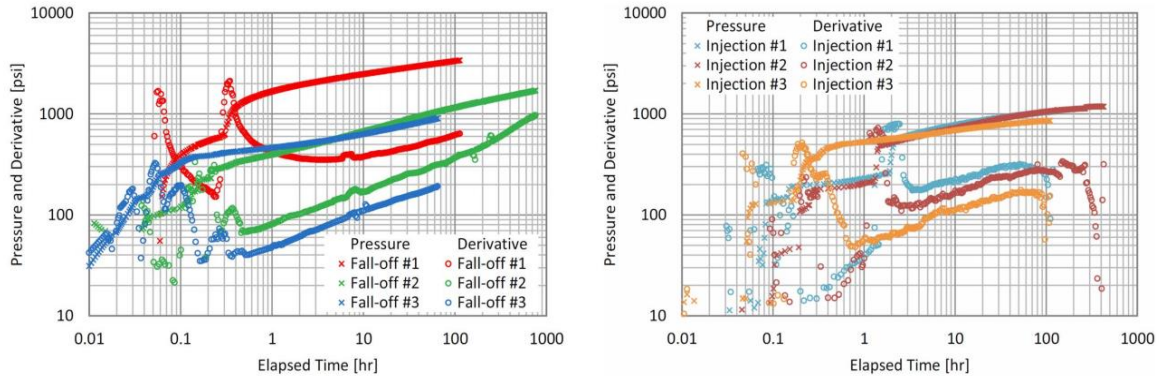

Figure 4. Time-lapse responses in pressure and derivative for fall-off (left) and injection(right) periods observed in history of a well (Shchipanov, 2014)

2.4 Data Acquisition and Quality Control (QC)

Pressure gauges have evolved since the first mechanical pressure transducers, later electronic gauges were introduced using strain sensors and also using a quartz transducer. (Kuchuk et al., 2010). Piezoelectric sensors such as Quartz or Sapphire crystals are very robust but are limited to a range of pressure and temperature in contrast with the gauges using optical sensors (Enyekwe & Ajienka, 2014). The most important metrological characteristics from the PTA perspective are the accuracy, drift and resolution provided that the other parameters are in order (Kuchuk et al., 2010).

Examples of metrology measurements from a Sapphire sensor and Quartz sensor in PDGs are shown in the Table 1. Example of gauges specifications and metrological characteristics. (Schlumberger(a), 2018, Schlumberger(b), 2018).

Table 1. Example of gauges specifications and metrological characteristics. (Schlumberger(a), 2018, Schlumberger(b), 2018)

Gauge performance	**Sapphire sensor**	**Quartz sensor**
Calibrated working pressure range, bar	689	689
Calibrated working temperature range, degC	25 to 110	25 to 130
Pressure accuracy, bar	± 0.1378 over full scale	± 0.2068 over full scale
Pressure resolution, bar	3.4 e-4	1.3 e-4
Pressure drift stability, bar	0.02 /year over full scale	0.2 /year over full scale
Temperature accuracy, degC	±0.5	±0.15
Temperature resolution, degC	±0.004	0.005
Temperature drift, degC	±0.1 per year at 100	±0.1 per year at 130

Additional to the conventional PDG, the fiber optic technology stands as an alternative to get accurate and long-term downhole P/T data in harsh environments. The benefits that can be encountered are the high resolution under high temperatures, high multidrop capability, low profile design (Halliburton, 2019).

Before proceeding to the analysis of the pressure responses, the preparation and validation of the raw data is needed.

In the preparation of the acquired data, some difficulties might be faced regarding rate history definition (well production history not complete or accurate requiring estimation or too many rate changes requiring simplification), error of start of the period when synchronizing the pressure and rate data (noisy pressure or oscillating at the time of shut-in), pressure gauge drift and pressure gauge noise. (Bourdet, 2002)

Some other important factors can affect the interpretation on the pressure responses that are produced by the well and reservoir condition. The effects generated that can be encountered are: the changing in wellbore storage (compressibility of fluid in wellbore is not constant, i.e. gas liberation from oil in the near-wellbore region); and the phase redistribution in wellbore during shut-in (a characteristic 'hump' is observed). These effects can be reduced by shortening the distance between the pressure gauge and the reservoir. In producing fields, the interference effects from production wells nearby can affect the analysis of the pressure data (Bourdet, 2002).

As mentioned by Bourdarot (1998), pressure measurements in an interference tests in the observation well while the pulse is generated in another well can be difficult to observe because of the weak signal measured (influence of tides effect) and the interference by other well that is not involved in the test as the signal occurs after a delay. In addition, he says that the little fluctuation that is always present in the producing wells could disturb the test.

In horizontal wells, the effective well length becomes important and estimating this value helps to reduce the uncertainty around this well parameter. Production logging is one of the methods to obtain the effective well length as well as the intelligent flow tracers.

The intelligent flow tracers quantify with high degree of accuracy the oil inflow contribution, water breakthrough monitoring and inflow assurance monitoring, while withstanding harsh downhole conditions and high pressures (Resman, 2018).

2.5 Reservoir simulation for analyzing interference tests

As stated by Gringarten & London (2008), the numerical simulation value for well tests analysis is in using the interpretation models obtained from PTA and verifying the results. However, he adds that the numerical modelling could help to identify the interpretation model accounting for various possible reservoir scenarios. Similarly, he mentions that well tests can contribute to characterize the reservoir and corroborate the reservoir model through consistency with the additional data.

As several interpretation models may be resulted from analytical PTA providing similar fit of the observations, the reservoir simulation can help in reducing the uncertainty with a model chosen. Numerical simulation can thus serve to improve the analytical model identification with matching more complicated reservoir behavior, not captured in analytical models. This may be achieved with history matching of a segment or full-field reservoir model, integrating the results from the analytical models (A. Shchipanov et al., 2017). The numerical models, accounting for new effects (like reservoir boundaries etc.), should match the same pressure

measurements. Overall, the analytical models are quite efficient in studying quickly different possible options to cover wide spread of reservoir uncertainty, while the scope of numerical models may then address cases with reduced uncertainty, but more reservoir and physical effects captured.

Analysis of interference test using a numerical modelling approach can be done, using a grid, and the model requires permeability as well as porosity and thickness distributions as input data, these may be taken from the analytical interpretation of interference tests (Bourdarot, 1998).

3. Field case

3.1 Geology

The field structure corresponds to a large northeast-southwest trending horst. Boundary sealing faults delimiting the field are established, but no internal faults evidence. The top seal is an upper Jurassic shale formation, with high organic content. The reservoir is divided in four flow units, the top layer is the main reservoir and is being produced by the horizontal wells, one of them is drilled partially into the underlaying layer. Both of these layers are partially connected according to the information acquired.

The main reservoir consists of mid-Jurassic sandstones with a light crude oil in the south. The formation presents a proximal-distal trend from South to North, and the thickness appears to be constant. A partially sealing layer between the main reservoir and the underlaying oil-bearing layer is determined. From core analysis, the porosity is approximately 0.15 in average and uniform along the reservoir, the permeability is less than 100 mD.

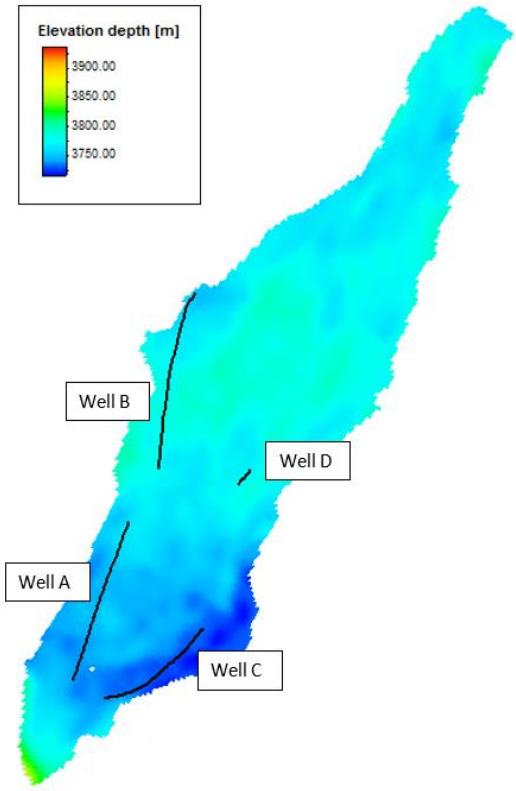

Figure 5. Top view of field. Only boundary faults.

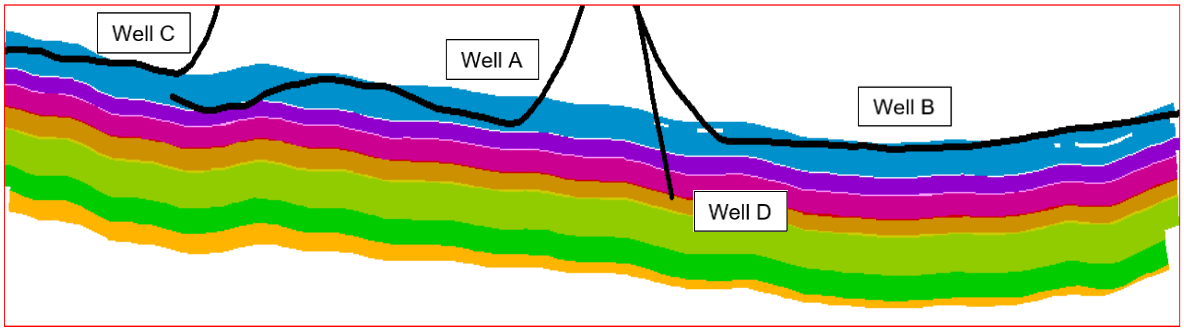

Figure 6. Cross section S-N.

The top view of the field can be observed in the Figure 5. Top view of field. Only boundary faults. The studied wells are in the southern part of the field, no internal faults were encountered and only boundary faults are present in the field. The S-N cross section shown in the Figure 6. Cross section S-N, illustrates the wells in the main layer (blue color) currently being produced; however, the well A is partially drilled into the layer below (purple color). As mentioned before, the connectivity between these two layers is low. The connectivity with the underlaying flow units is nonexistent as a sealing layer separates the two upper most layers to the ones below.

3.2 Well locations and completions

The wells considered in this thesis are located in the southern part of the field, three horizontal production wells and one deviated injection well. The horizontal wells are open hole with sand screens and Passive Inflow Control Devices (ICDs) to equalize the flux along the horizontal section, a schematic of the well is shown in the Figure 7. Schematic of horizontal well completion of producing wells. The PDGs are installed above the reservoir, 150 meters in average for the production wells. Oil and water chemical inflow tracers were installed.

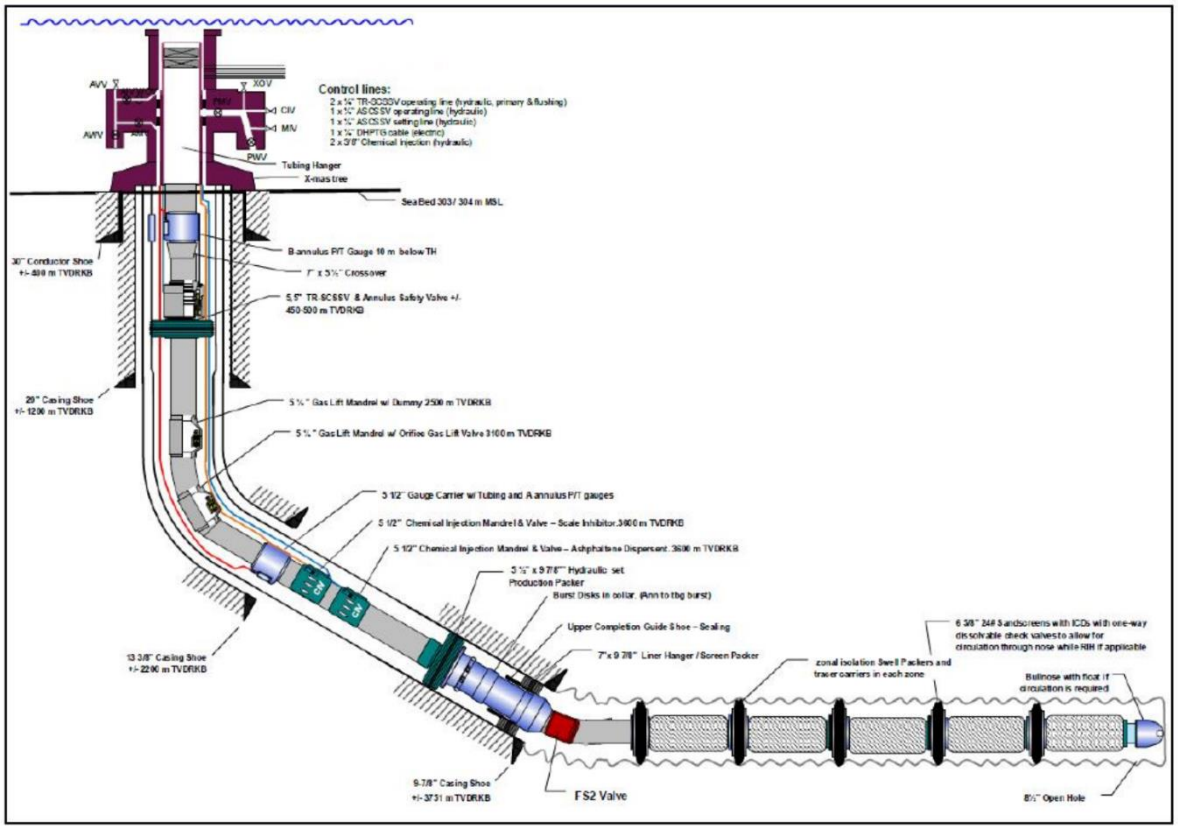

Figure 7. Schematic of horizontal well completion of producing wells.

3.3 Production history

The reservoir started with initial pressure at 391 bara, according to the PVT results the bubble point pressure is about 216 bara. The production wells start producing above the saturation pressure. Production history includes last 2 years of field production.

The production and pressure history along time for well A, B, and C is shown in the Figure 8.History plot for well A. Pressure data at PDG, bara (top); and oil rate, m3/D (bottom) vs time, hr. the Figure 9. History plot for well B. Pressure data at PDG, bara (top); and oil rate, m3/D (bottom) vs time, hr., and the Figure 10. History plot for well C. Pressure data at PDG, bara (top); and oil rate, m3/D (bottom) vs time, hr., respectively. As it can be observed from the history plots, for each well, the last two PBUs are below the bubble point pressure at the PDGs and probably below or very close to it in the near-wellbore region.

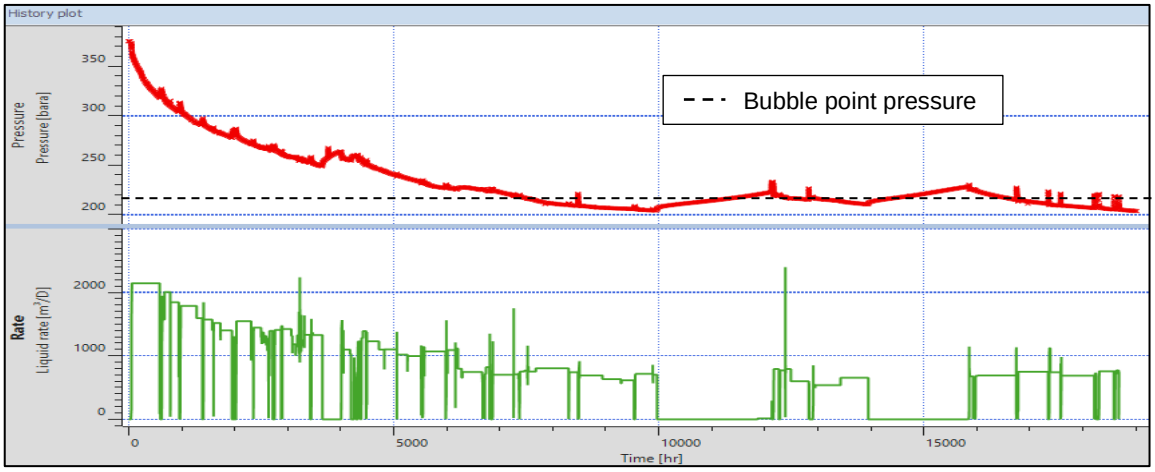

Figure 8.History plot for well A. Pressure data at PDG, bara (top); and oil rate, m3/D (bottom) vs time, hr.

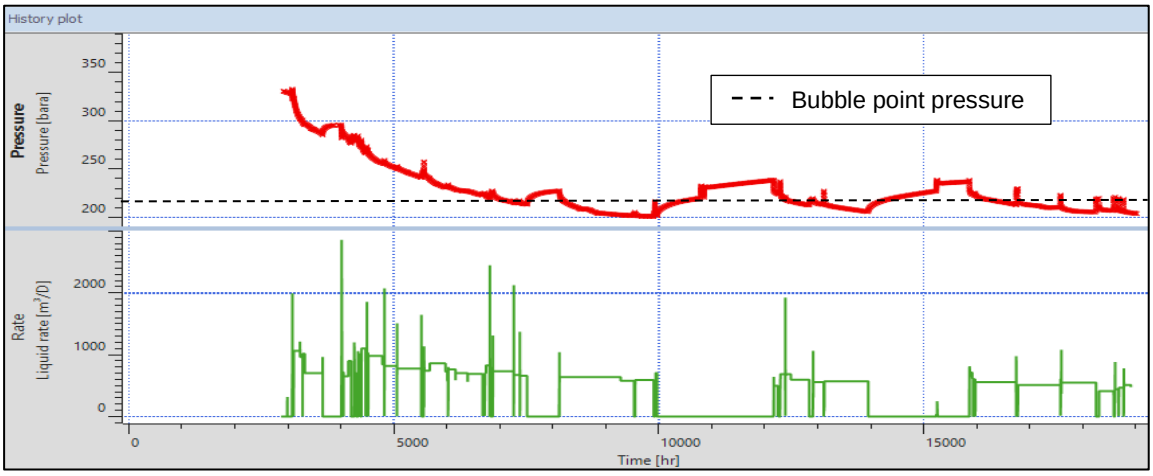

Figure 9. History plot for well B. Pressure data at PDG, bara (top); and oil rate, m3/D (bottom) vs time, hr.

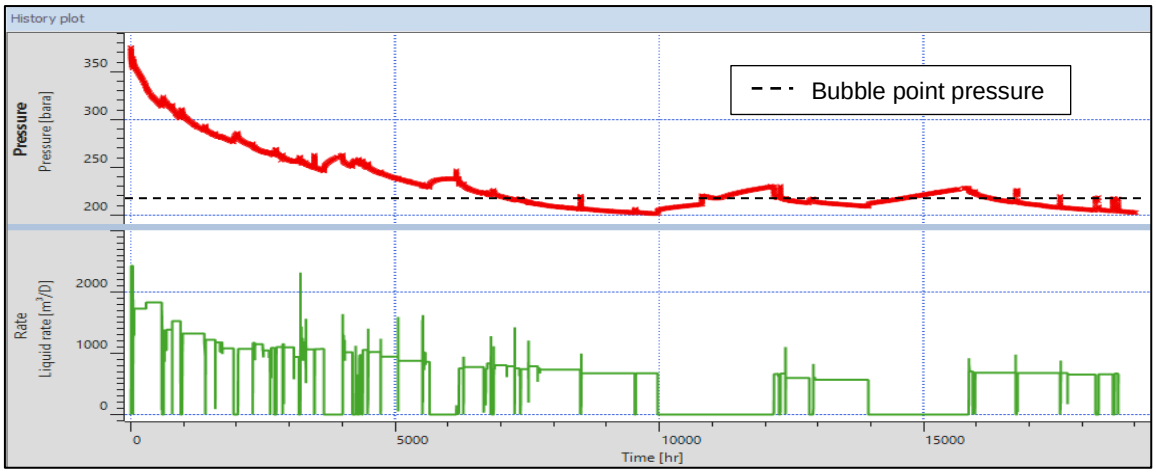

Figure 10. History plot for well C. Pressure data at PDG, bara (top); and oil rate, m3/D (bottom) vs time, hr.

The combined well history is presented in the Figure 11. History plot for all production wells. Pressure data at PDG, bara (top); and oil rate, m3/D (bottom) vs time, hr. The well A and C started production at about the same time, and after 3000 hr or 4 months later, the well B stars to produce. As the reservoir pressure declines, getting closer to the bubble point pressure, water injection in the field is implemented to increase the pressure within the reservoir about 8000 hr or 11 months after start of the production.

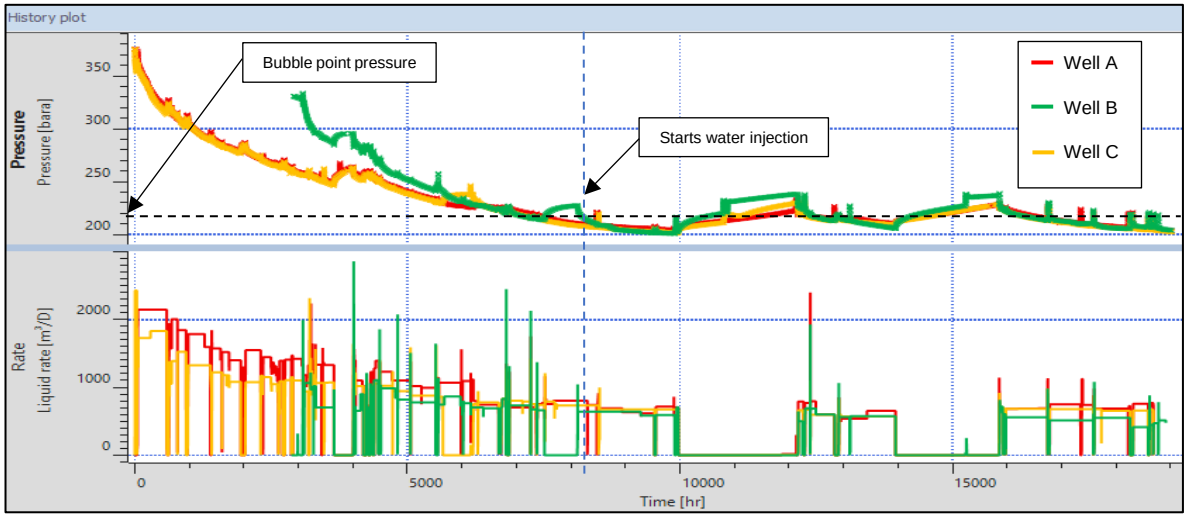

Figure 11. History plot for all production wells. Pressure data at PDG, bara (top); and oil rate, m3/D (bottom) vs time, hr.

3.4 Challenges with field production

Long horizontal wells drilled in the field, between 1,5 and 2,5 km length, are supported by one slanted injector which was started almost a year after the start of production The oil field experiences faster decline in pressure than expected due to insufficient pressure support, getting close to the bubble point pressure. There is a high uncertainty on the measured reservoir bubble point pressure in the field making it challenging to understand the well behavior. As the bottom hole pressure is below the Pb, the PTA will show a higher value of the skin factor as a result of the increase in the gas saturation in the near-wellbore region and the reduction in the oil relative permeability.

The results from chemical tracers showed reduction in effective well length with time which is not in line with PI development of the wells. Comparison to effective well length from PTA can prove or verify opposite observed from tracers analysis.

4. Methodology

The present work involves the analysis of interference test as a part of time-lapse PTA interpretations for horizontal wells using the data from permanent downhole gauges (above formation) and flow rate measurements at the surface. Applicability of the classical methods for interference test interpretation is limited here due to well completion design and locations: long horizontal wells located at comparatively short (smaller than the well lengths) distance from each other. First, analytical models are applied to analyze well responses; secondly, numerical model analyses are carried out in 2D; and finally, 3D full-field numerical analysis is performed to evaluate the reservoir production. These analyses were completed using the software Saphir from KAPPA Engineering.

The study has the following structure:

- Analytical 2D models. Here, the log-log pressure and the derivative plot is used to get the first estimates of the interpretation model. The analysis is made for the pressure buildup data from each well with the main objective of characterizing the reservoir around the well and identify interference with other wells. PBUs before water injection had started in the field and after it are analyzed.
- Numerical 2D Model. After the analytical model phase, a numerical analysis (2D) is made using unstructured grids (PEBI) in Saphir, from KAPPA. The process is carried out for the main layer (top layer) of the reservoir which is being produced, considering producers and injectors.
- Numerical 3D Model. After the numerical modelling 2D using Saphir, a full description of the reservoir is made using the results from the previous studies. A more robust multi-layer numerical model (3D) is implemented using Saphir software from KAPPA. The input data required for the study are the permeability, porosity and thickness distributions. The 3D study is implemented because there is some uncertainty on the contribution from the lower zone of the main layer or the underlaying oil-bearing layer.

5. Analytical models: Interpretation and simulation results

5.1 Analytical model set-up

A reference model was established for the analysis using analytical models. The horizontal wells and the injection well are placed in a closed chamber (rectangle) based on an approximation to the real field geometry, as established from seismic, and considering proper well locations and similar PV. The Figure 12. Sketch of the field and approximated shape (rectangle) of closed system. shows the rectangular shape to be used in the analytical models and the real reservoir geometry.

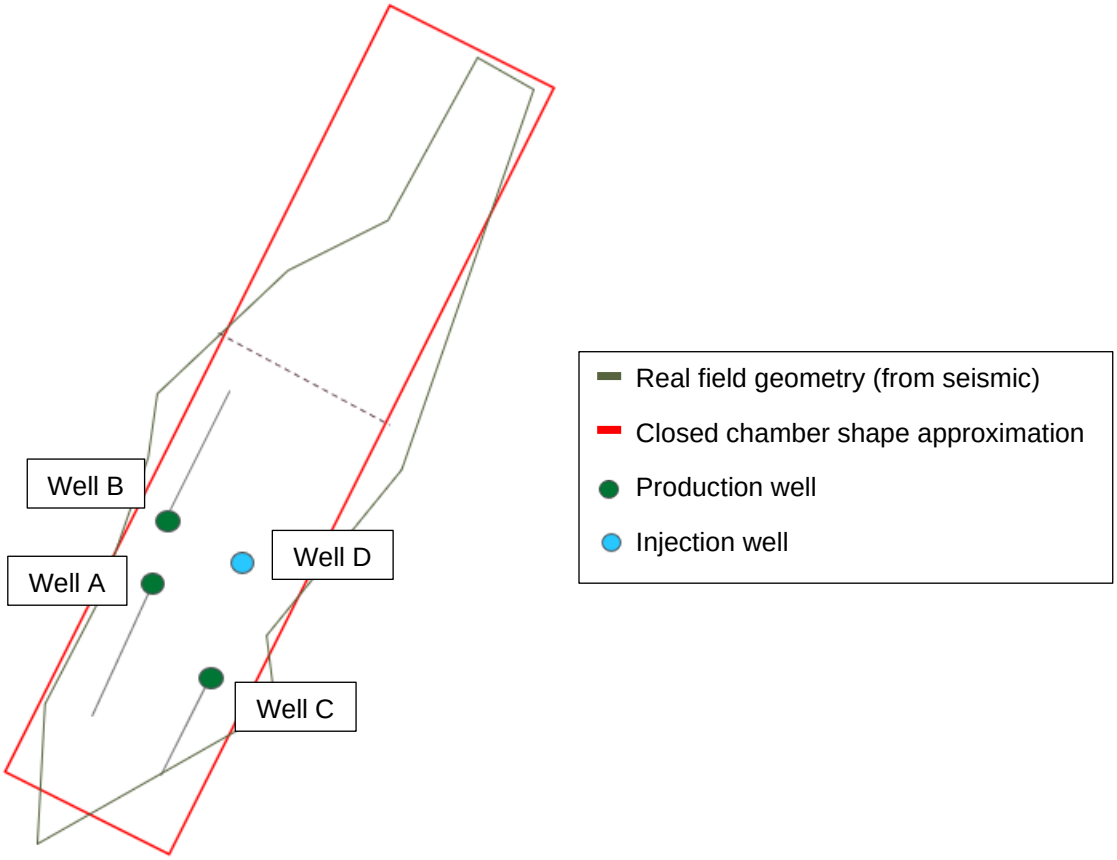

Figure 12. Sketch of the field and approximated shape (rectangle) of closed system.

The reservoir and fluid properties used in the reference model for the analytical models are shown in the Table 2. Reservoir and fluid properties for the reference model. These were obtained from estimated values from PVT analysis, core analysis, well logging for the studied field. The used effective horizontal well lengths for each producing well in the analytical models were selected according to the estimates from the chemical PLT data.

Table 2. Reservoir and fluid properties for the reference model.

Parameters	Value	Units
Pi	391	bara
kh	960	md.m
k	80	md
h	12	m
k_v/k_h	0.05	fraction
ϕ	0.15	fraction
cr	8.20E-05	bar-1
co	2.17E-04	bar-1
cw	4.00E-05	bar-1
ct	2.72E-04	bar-1

5.2 Sensitivity analysis on example of well A

The parameters that characterize the well and the reservoir have either a higher or lower degree of uncertainty. The sensitivity analysis to permeability, thickness, k_v/k_h, and total compressibility within the reservoir parameters and the effective well length, wellbore storage coefficient, and skin factor within the well parameters is carried out to evaluate the impact of these on the pressure difference and the pressure derivative in the log-log plot. The reservoir and well parameters sensitivity analysis is shown in the Figure 13. Sensitivity analysis plots to reservoir parameters: permeability (top left), kv/kh (top right), total compressibility (bottom left), formation thickness (bottom right). and Figure 14. Sensitivity to well parameters, effective well length (top left), Skin factor (top right), and wellbore storage coefficient, C (bottom left)., respectively.

The sensitivity analysis indicates how an increase in the permeability, thickness, ct, and effective well length shift the derivative down. A high value of wellbore storage coefficient, low value of k_v/k_h, and a high skin factor mask the first radial flow observed in the horizontal wells.

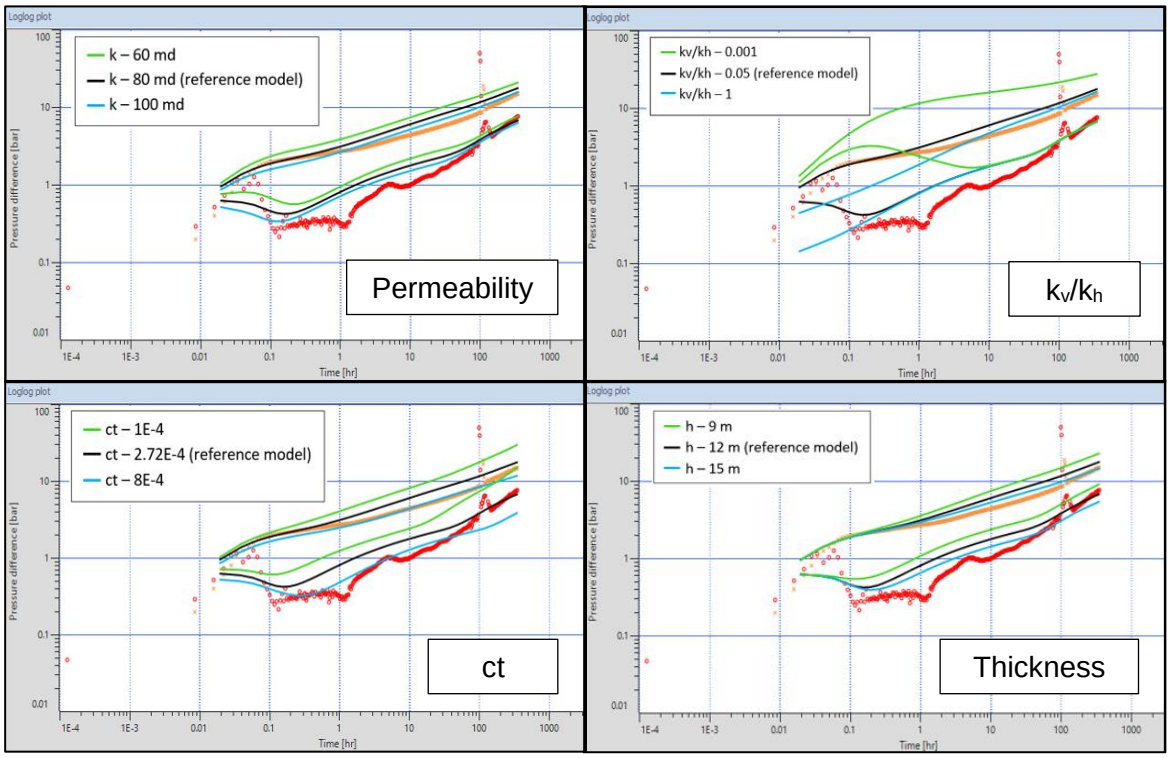

Figure 13. Sensitivity analysis plots to reservoir parameters: permeability (top left), kv/kh (top right), total compressibility (bottom left), formation thickness (bottom right).

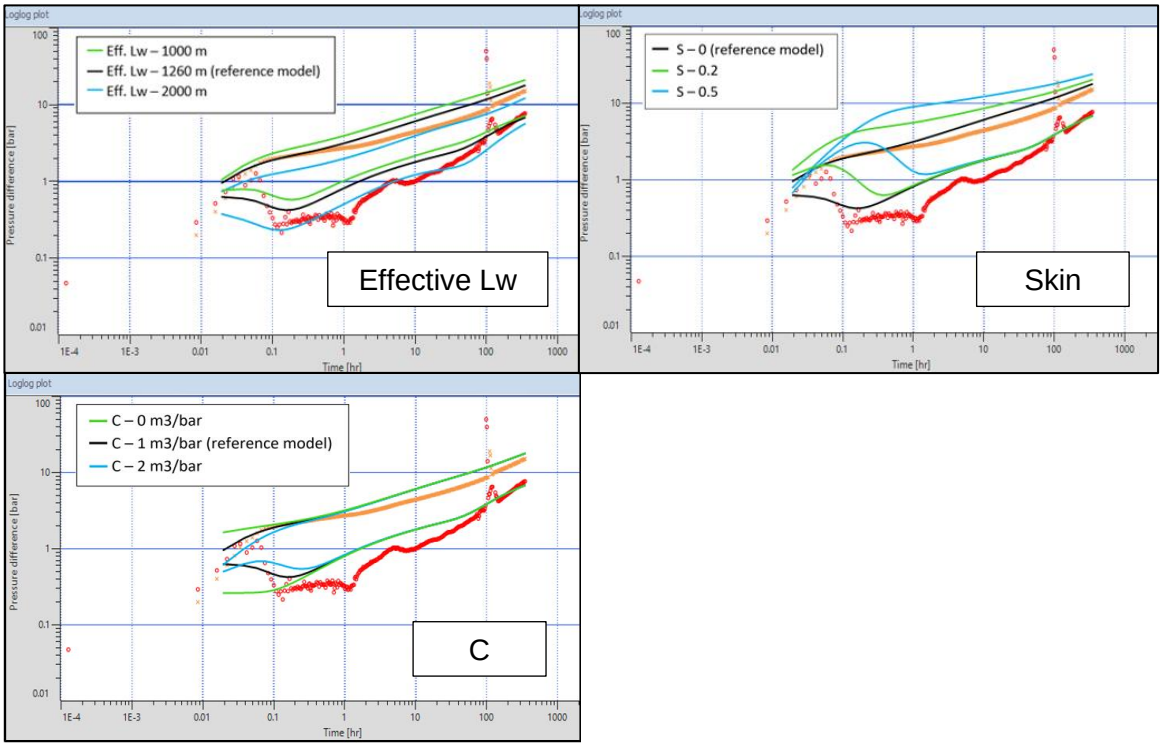

Figure 14. Sensitivity to well parameters, effective well length (top left), Skin factor (top right), and wellbore storage coefficient, C (bottom left).

5.3 Analysis workflow

The aim of the analysis is to study the well interference between producers and producer-injector, evaluate the impact of water injection and the well performance in the effective well length. The analysis with analytical models is carried out first for a well without the interference of nearby wells (single well model); second, the effect of only the producing wells nearby (all producing wells case) is studied; then, the introduction of the water injection well (introducing water injection case) is considered. On top of it, the sensitivity to effective well length based on PLT is studied for the first PBU. Finally, the reduction of the distance to the north boundary is analyzed only for well B. The process is summarized in the Figure 15. Analytical analysis workflow

The analysis with analytical model for the case including the nearby horizontal producing wells requires the assumption of replacing the surrounding wells by the line-source well solution to account for the possible interference with the neighbor wells. The location of the points representing the nearby horizontal wells is selected close to the center of the horizontal section.

Figure 15. Analytical analysis workflow

5.4 Well A

The well A started production in the field at about the same time as well C and before the well B. The well is located in the south west of the south compartment. Water injection starts approximately 8000 hours after the field starts producing. Three suitable pressure buildups for analysis are obtained from the data from the PDGs. For the first PBU all the three wells are producing and are shut-in for 13 days approximately, no water injection at that time. During the second and third PBU, all the production wells, A B and C, are shut-in, and the water injection well, D, has been injecting for several months.

The Figure 16. Time-lapse log-log plot (top) and history plot (bottom) for well A. shows the time-lapse pressure derivatives for well A. The vertical radial flow regime, common in horizontal wells, is seen only for the first PBU. The second and third PBU pressure derivatives exhibit similar behavior as both are shifted down slightly compared to the first PBU. These two PBUs show large effects of phase redistribution (gas and oil) in the early-

time region as a result of lower pressures than the bubble point pressure at the gauges and possibly in the reservoir. No late pseudo-radial flow regime appearing in the derivatives as the transient is affected by the interference with the wells nearby and or boundaries encountered before developing the regime.

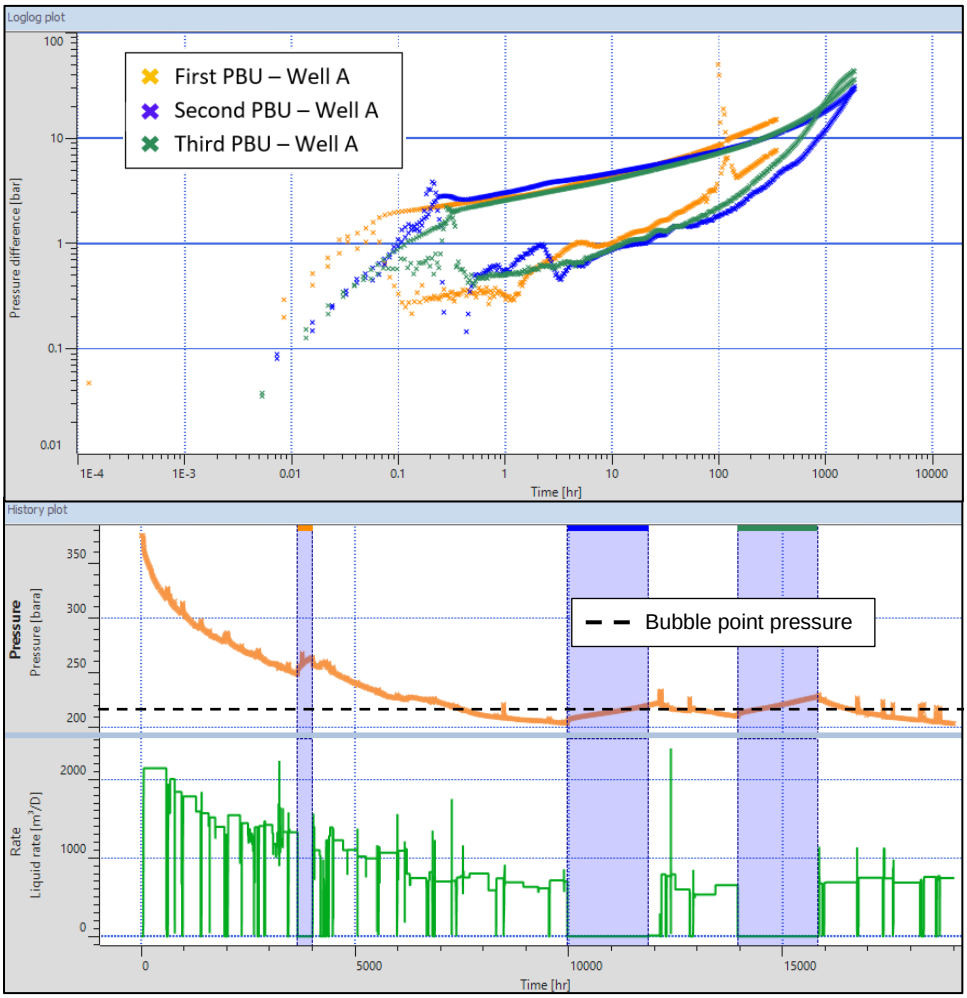

Figure 16. Time-lapse log-log plot (top) and history plot (bottom) for well A.

- **First PBU – Well A**

In the first PBU for the well A, the three production wells were producing before the shut-in and all three were shut-in concurrently. No water injection in the field at the time of the first PBU. The analytical results considering the single well model, only production wells model, and the case including producers and injector are observed in the Figure 17. Analytical model results for single well case, all production wells and introducing water injection well case for well A, first PBU. Derivative (top) and history plot (bottom). The modeled derivatives

adjust slightly using the reference model for the reservoir properties and distance to boundaries.

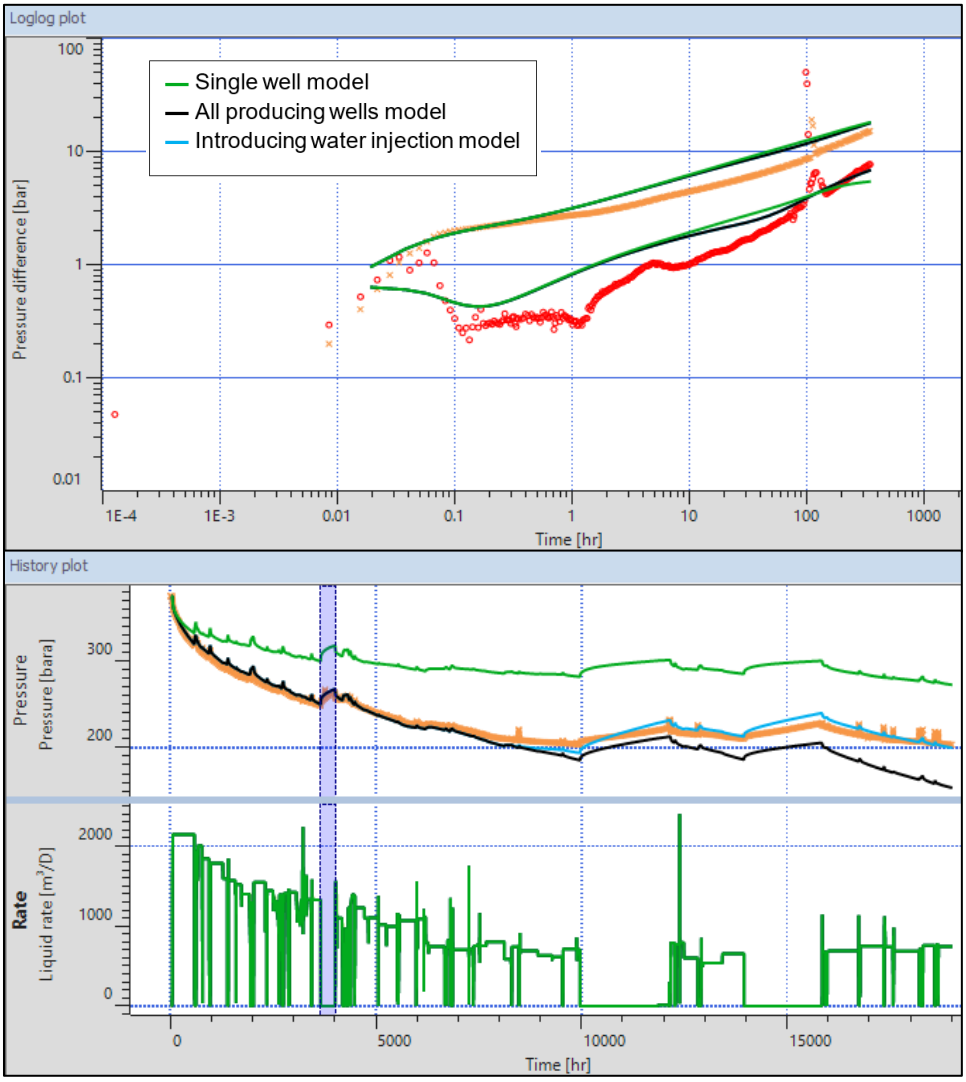

Figure 17. Analytical model results for single well case, all production wells and introducing water injection well case for well A, first PBU. Derivative (top) and history plot (bottom).

The single well model does not describe the behavior of the derivative at late-time region in comparison to the cases considering the producing wells. This shows that there could be hydraulic communication between the producers. The model introducing water injection only affects the history plot and it can be observed that it supports pressure and reduces the pressure declination as observed in the field.

The sensitivity to effective well length based on estimated values from the PLT results is shown in the Figure 18. Sensitivity to effective well length for well A based on PLT. Derivative

plot (top) and history plot (bottom). The reference model has a low value compared to the drilled horizontal section. The three cases considered where generated using all producers and injector model. The plot shows that an increased effective well length shifts down the modeled derivative and that a value around 1700 m of effective well length could describe better the response.

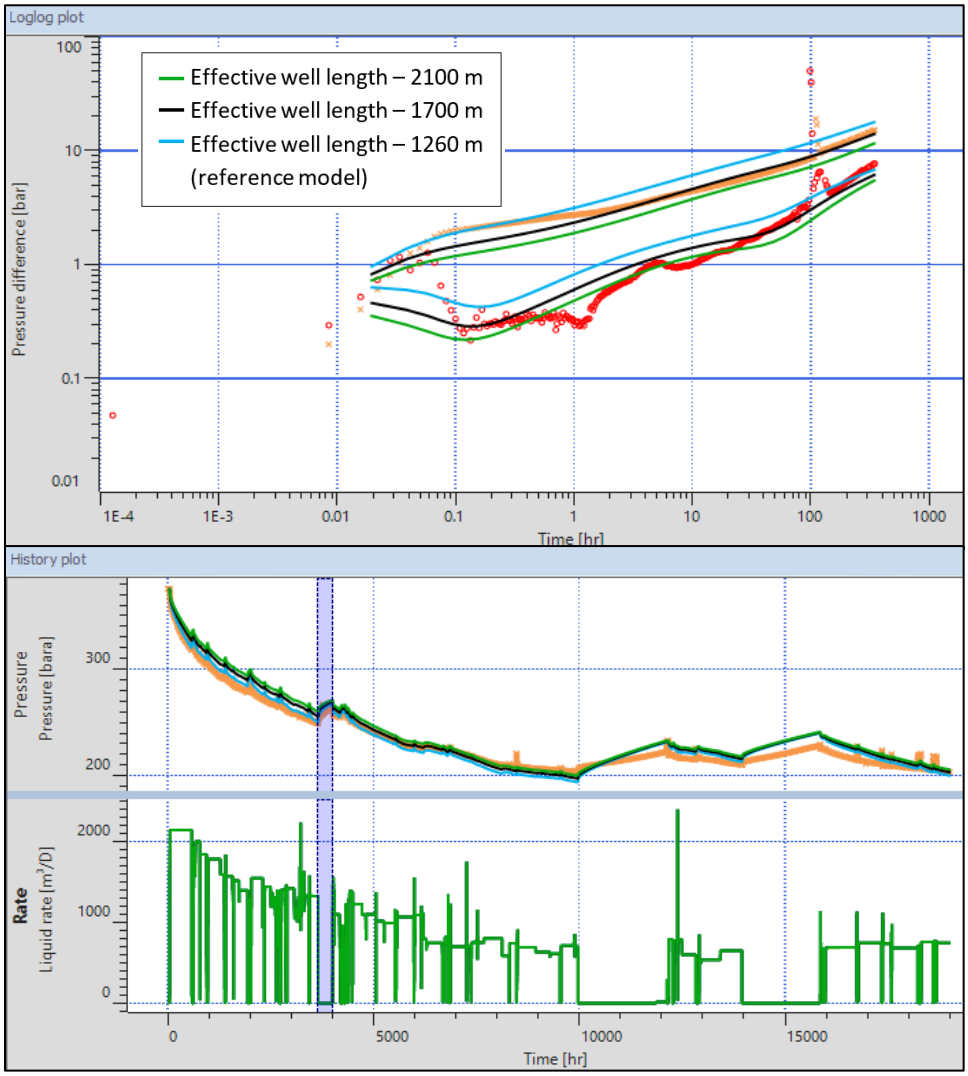

Figure 18. Sensitivity to effective well length for well A based on PLT. Derivative plot (top) and history plot (bottom).

- **Second PBU – Well A**

In the second PBU for the well A, the three production wells were producing before the shut-in and all three were shut-in concurrently. Water injection in the field has already started before the second PBU. The analytical results considering the single well model, only production wells model, and the case including producers and injector are observed in the

Figure 19. Analytical model results for single well case, all production wells and introducing water injection well case for well A, second PBU. Derivative plot (top) and history plot (bottom)., the modeled derivatives are shifted up suggesting that the well A could have experienced an increase in effective well length or contribution of an underlying formation that increases the kh compared to the previous PBU.

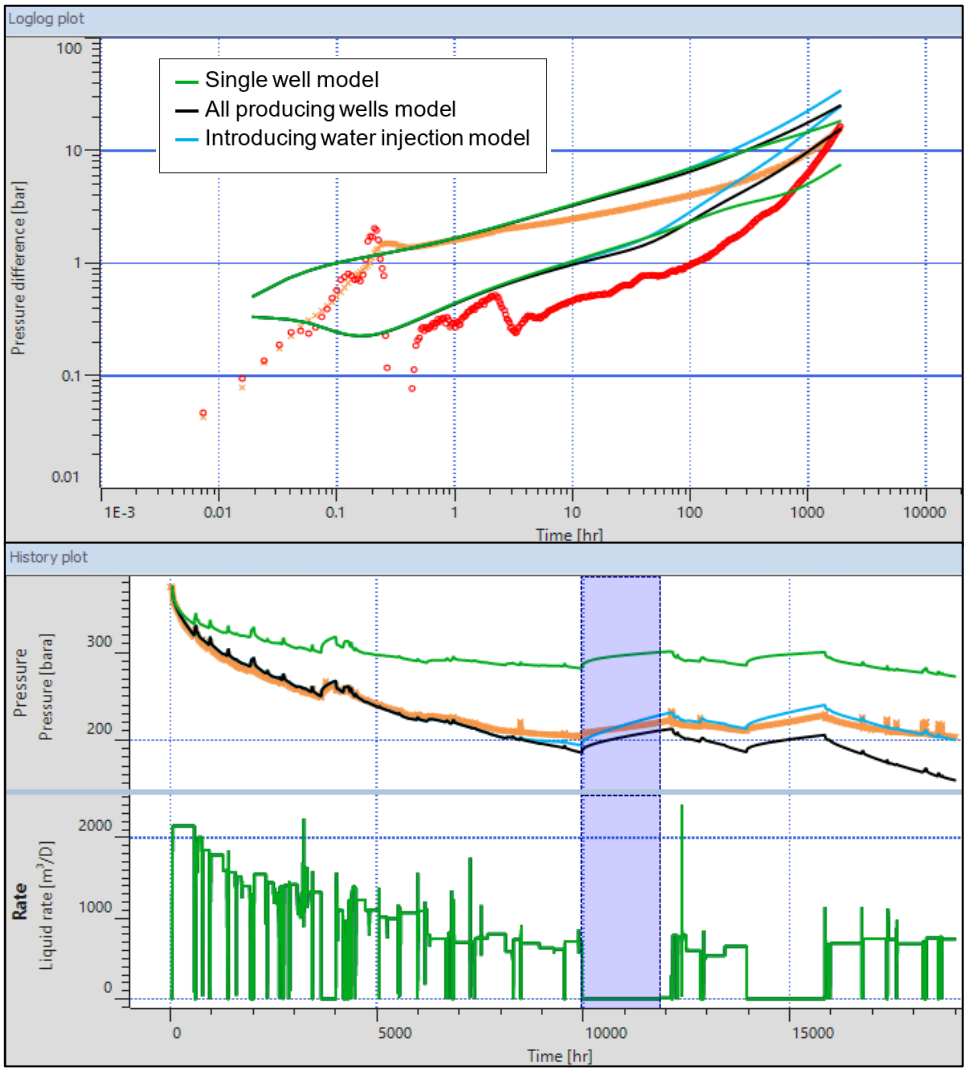

Figure 19. Analytical model results for single well case, all production wells and introducing water injection well case for well A, second PBU. Derivative plot (top) and history plot (bottom).

The model that best describes the derivative in the late-time region is the case that introduces the water injector compared to the single well model and all producers model. The injection accounts for the support in pressure observed in the history plot. This suggests hydraulic communication between the well A and the injection well D.

Increasing effective well length model, well A and second PBU.

A possible reason of the shifting down of the derivative after water injection could be an increase in the effective well length from 1260 m. However, to get a closer match of the pressure derivative it is required an increase of this parameter to 3000 m, the log-log plot reflecting this change is shown in the Figure 20. Increased effective well length to 3000 m for well A and second PBU. If we consider that the drilled horizontal section for this well is 2100 m, and an increase in 900 m could not be used based on the data obtained, then it is possible that is the result of an increase in the flow capacity of the reservoir due to an increase in the permeability or the additional thickness contributing.

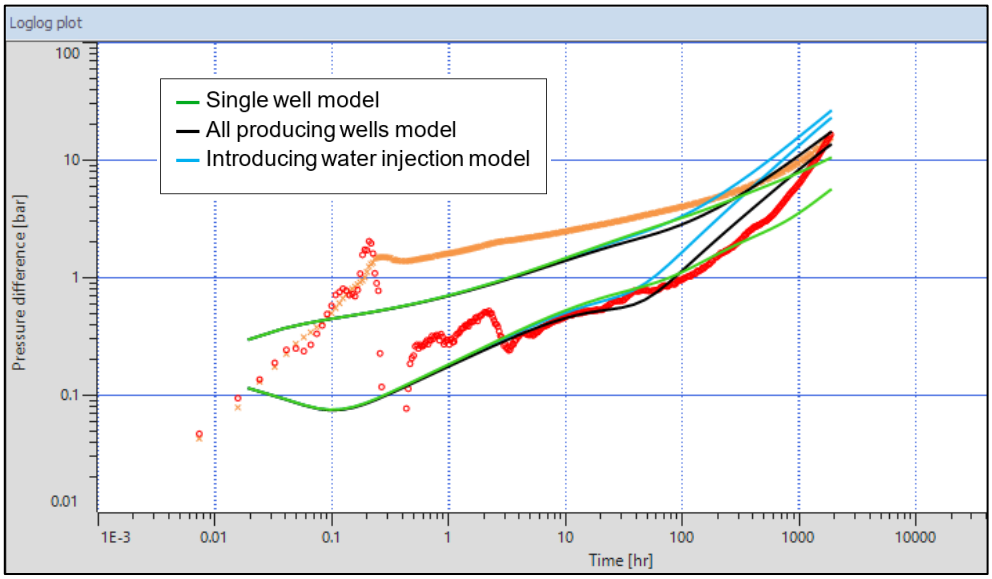

Figure 20. Increased effective well length to 3000 m for well A and second PBU.

- **Third PBU – Well A**

In the third PBU for the well A, the three production wells were producing before the shut-in and all three were shut-in concurrently. Water injection in the field has already started before the third PBU. The analytical results considering the single well model, only production wells model, and the case including producers and injector are observed in the Figure 21. Analytical model results for single well case, all production wells and introducing water injection well case for well A, third PBU. Derivative (top) and history plot (bottom). The modeled derivatives are shifted up with the same proportion as the second PBU as shown in the Figure 16. Time-lapse log-log plot (top) and history plot (bottom) for well A. , this suggests that the well A could have experienced an increase in effective well length or contribution of an underlying formation that increased the kh compared to the first PBU.

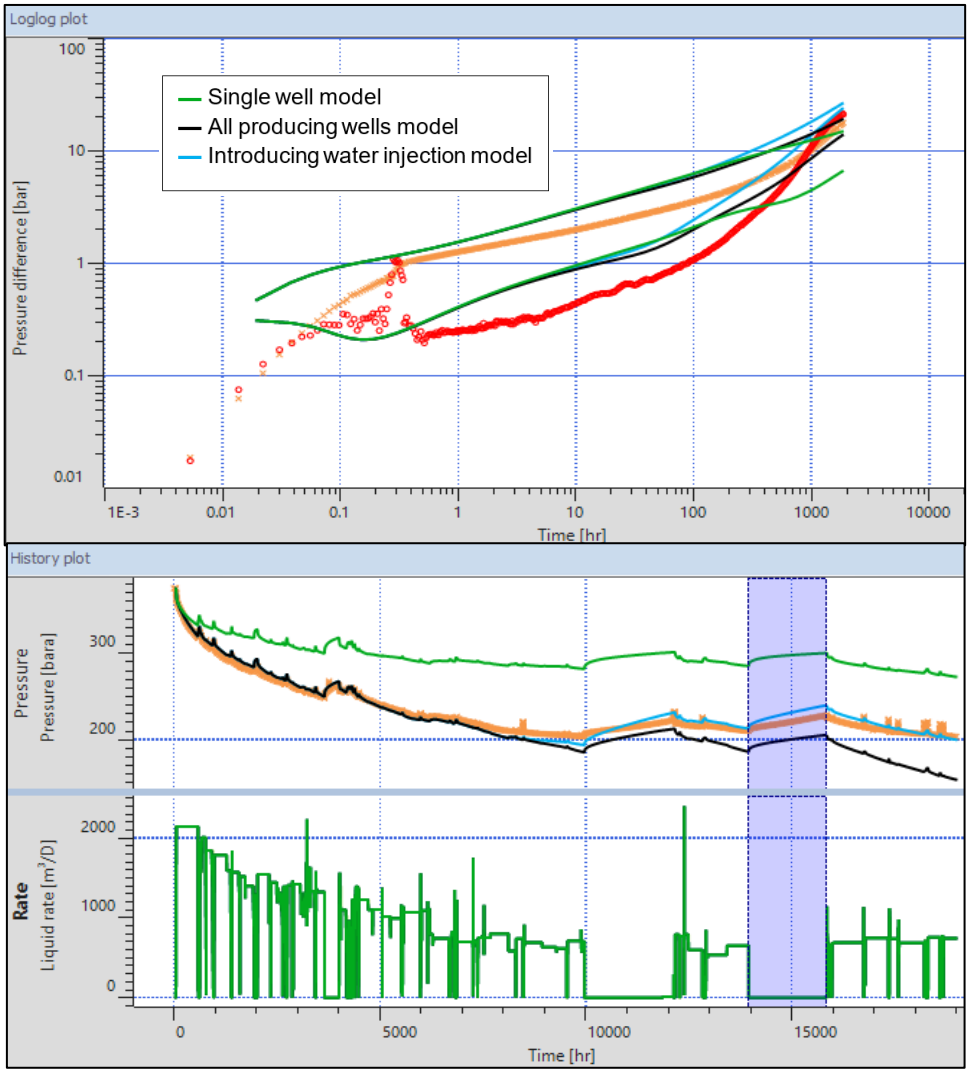

Figure 21. Analytical model results for single well case, all production wells and introducing water injection well case for well A, third PBU. Derivative (top) and history plot (bottom).

The model that best describes the derivative in the late-time region is the case that introduces the water injector compared to the single well model and all producers model. The injection accounts for the support in pressure observed in the history plot. This suggests hydraulic communication between the well A and the injection well D.

5.5 Well B

The well B started production about 5 months after the producers nearby started to produce in the field. The well is located in the north of the south compartment. Water injection starts during the last months of 2018. Four suitable pressure buildups for analysis are obtained

from the data from the PDGs. For the first PBU all the three wells are producing and are shut-in for 13 days approximately, no water injection at that time. The second PBU corresponds to the interference test, where the well B (observation well) is shut-in and the nearby wells are kept producing at a constant rate. During the third and fourth PBU, all the production wells, A, B and C, are shut-in, and the water injection well, D, has been injecting for several months.

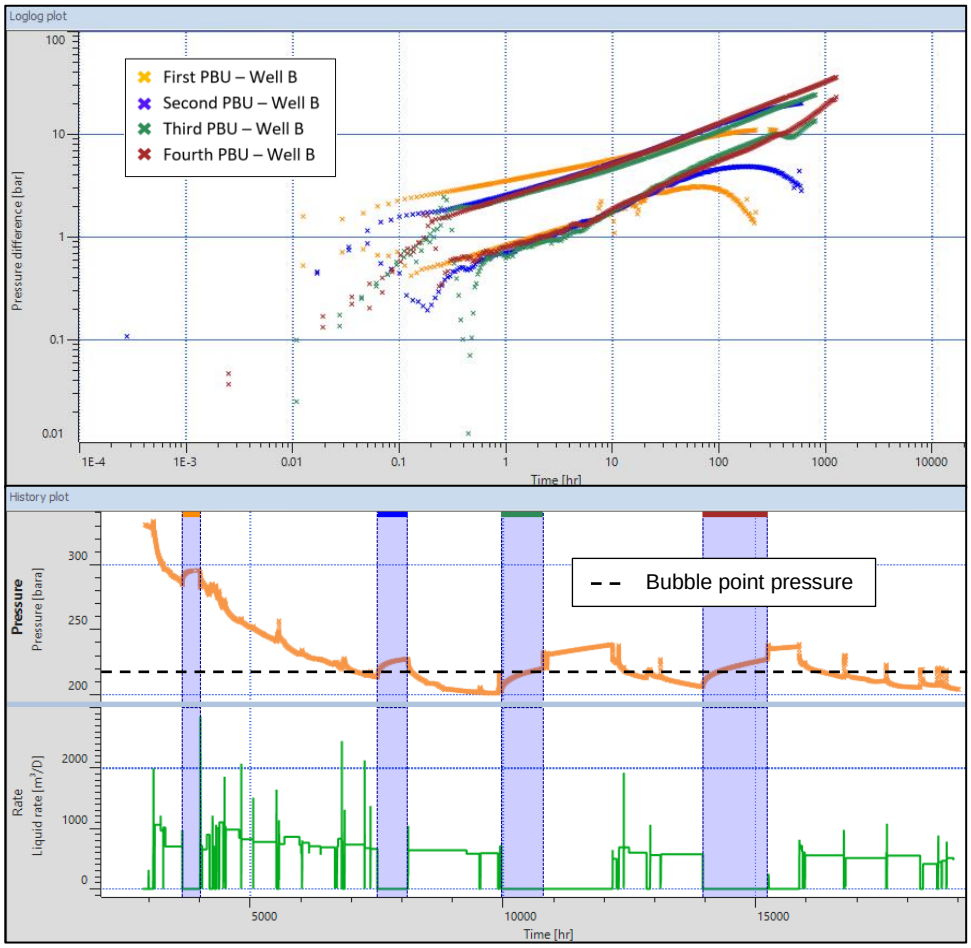

Figure 22. Time-lapse log-log plot (top) and history plot (bottom) for well B.

The Figure 22. Time-lapse log-log plot (top) and history plot (bottom) for well B. shows the time-lapse pressure derivatives for well B. The early radial flow regime, common in horizontal wells, is not seen in any of the pressure buildup periods. The first and second PBU pressure derivatives exhibit similar behavior at the late-time region.

The derivative of the second PBU going down, characteristic of a steady state flow, is explained by the well interference caused by the production of the nearby wells. However, for the first PBU, with all the producers shut-in as in the third and fourth PBU; the similar derivative response to the second PBU is the result of the depletion of the area by the production of the nearby horizontal wells that started to produce about 4 months before well B. This effect is later attenuated and is not observed in the late-time region of the third and fourth PBU.

In the early-time region, larger effects of phase redistribution (gas and oil) for the PBUs after water injection, shown in the Figure 22. Time-lapse log-log plot (top) and history plot (bottom) for well B., as a result of lower pressures than the bubble point pressure at the gauges and possibly in the reservoir. No late pseudo-radial flow regime appearing in the derivatives as the transient is affected by the interference with the wells nearby and/or boundaries encountered before developing the regime.

- **First PBU – Well B**

In the first PBU for the well B, the three production wells were producing before the shut-in and all three were shut-in concurrently. No water injection in the field at the time of the first PBU. The analytical results considering the single well model, only production wells model, and the case including producers and injector are observed in the Figure 23. Analytical model results for single well case, all production wells and introducing water injection well case for well B, first PBU. Derivative (top) and history plot (bottom). The modeled derivatives are shifted down suggesting that the well B could have lower effective well length or a lower flow capacity reservoir zone compared to the values from the reference model.

The single well model does not describe the behavior of the derivative at late-time region in comparison to the cases considering the producing wells. This shows that there is hydraulic communication between the producers. The model introducing water injection only affects the history plot and it can be observed that it supports pressure and reduces the pressure declination as observed in the field.

The sensitivity to effective well length based on estimated values from the PLT results is shown in Figure 24. Sensitivity to effective well length for well B based on PLT. Derivative plot (top) and history plot (bottom). The reference model has a high value closed to the drilled horizontal section. The three cases considered where generated using all producers and injector model.

The plot shows that a reduced effective well length shifts up the modeled derivative but not enough in the values considered to explain the response.

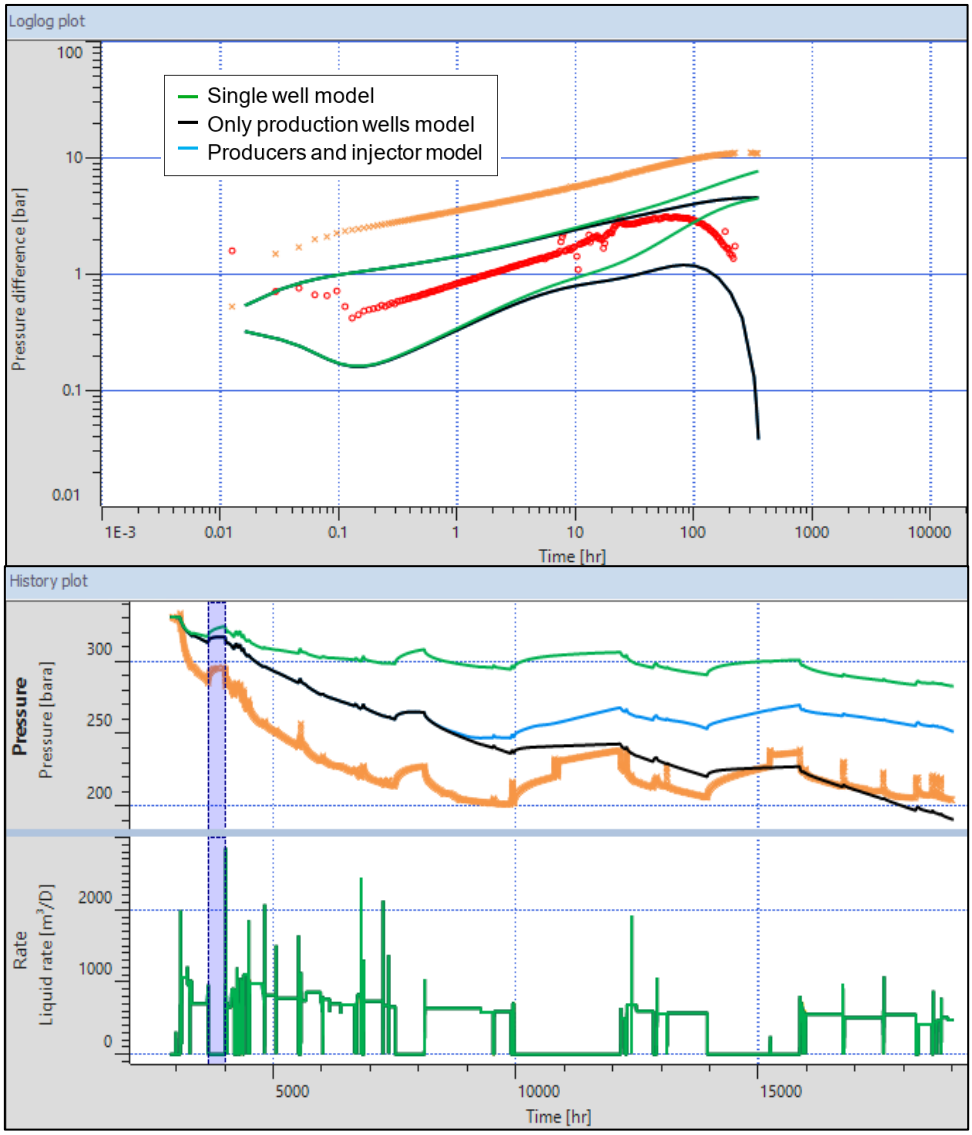

Figure 23. Analytical model results for single well case, all production wells and introducing water injection well case for well B, first PBU. Derivative (top) and history plot (bottom).

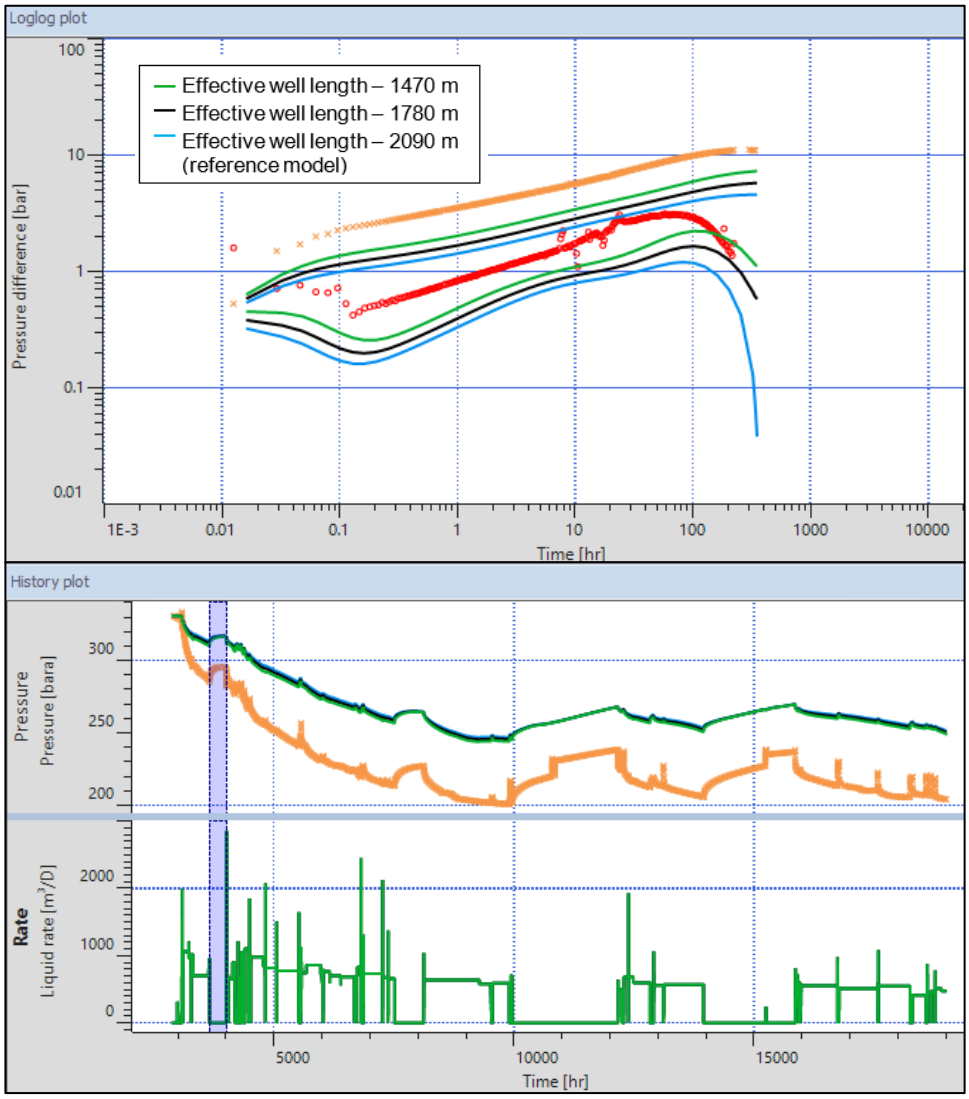

Figure 24. Sensitivity to effective well length for well B based on PLT. Derivative plot (top) and history plot (bottom).

The distance between the well B and the boundary to the north was reduced representing a reduction of 38% of the pore volume and including the effects of the other wells neaby. The results are shown in the Figure 25. Analytical model results for all production wells, introducing water injection well case and reduced boundary including water injection well for well B, first PBU. Derivative plot (top) and history plot (bottom)., where the reduced boundary model is compared with all production wells model, and producers and injector model. The reduced boundary case increases the declination of the pressure.

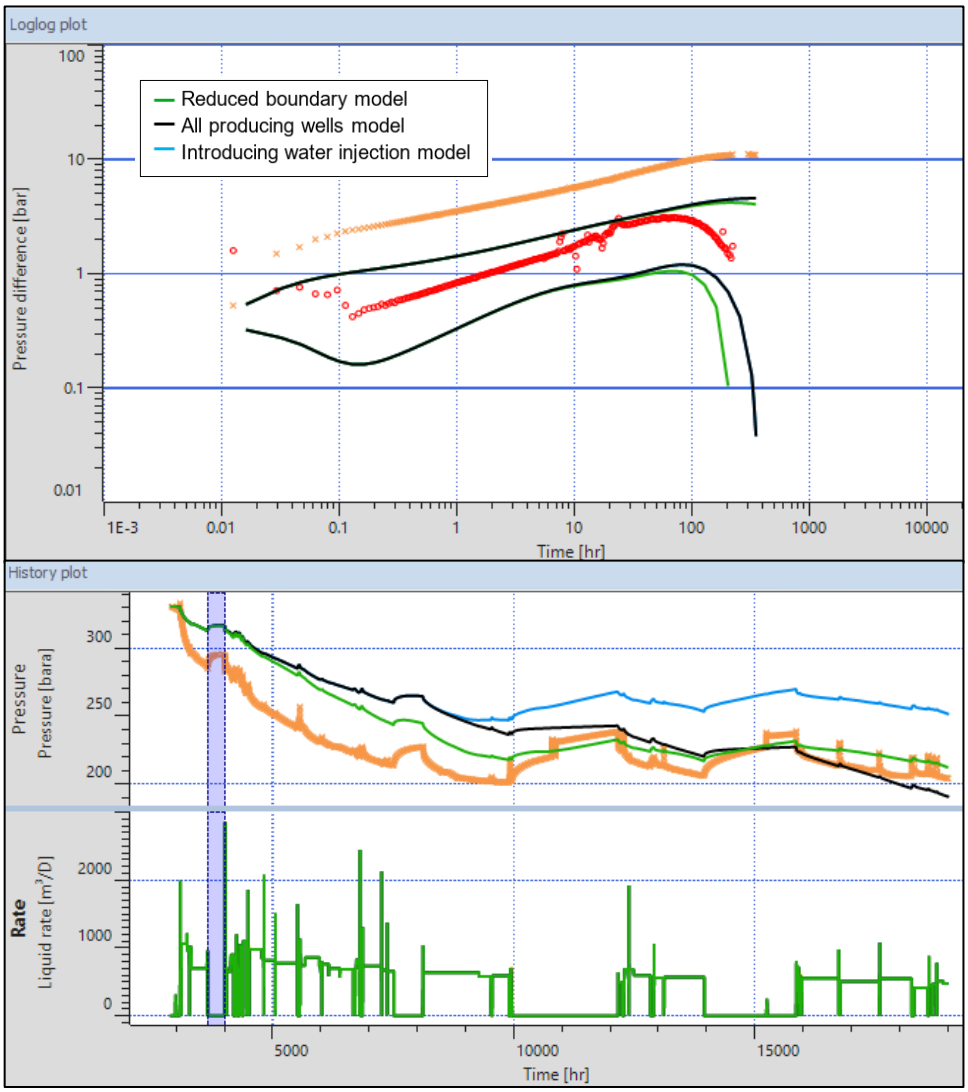

Figure 25. Analytical model results for all production wells, introducing water injection well case and reduced boundary including water injection well for well B, first PBU. Derivative plot (top) and history plot (bottom).

- **Second PBU – Well B**

The second PBU for the well B corresponds to the interference test. The producing wells nearby, A and C, were producing along with well B before the shut-in of well B (observation well); however, well A and C (active wells) keep producing during the PBU of B. No water injection in the field at the time of the second PBU. The analytical results considering the single well model, only production wells model, and the case including producers and injector are observed in the Figure 26. Analytical model results for single well case, all production wells and introducing water injection well case for well B, second PBU. Derivative plot (top) and history plot (bottom). The modeled derivatives are shifted down suggesting that the well B could have lower effective well length or a lower flow capacity reservoir zone compared to the values from the reference model as in the first PBU.

The single well model does not describe the behavior of the derivative at late-time region in comparison to the cases considering the producing wells. This suggests that there is communication between the producers. The model introducing water injection only affects the history plot and it can be observed that it supports pressure and reduces the pressure declination as observed in the field.

- **Third PBU – Well B**

In the third PBU for the well B, the three production wells were producing before the shut-in and all three were shut-in concurrently. Water injection in the field has already started before the third PBU. The analytical results considering the single well model, only production wells model, and the case including producers and injector are observed in the Figure 27. Analytical model results for single well case, all production wells and introducing water injection well case for well B, third PBU. Derivative (top) and history plot (bottom). The modelled derivatives are shifted down suggesting that the well B could have lower effective well length or a lower flow capacity reservoir zone compared to the values from the reference model as in the previous PBUs.

This transient period corresponds to a multi-well interference test, being well D (the injection well) the active well, and well A, B, and C the observation wells. The active well is injecting while the observation wells are shut-in, and after some time, the injection rate changes significantly generating the pulse to be observed in the observation wells.

The model with all producing wells, without considering the injection well, does not describe the behavior of the derivative at middle and late-time region in comparison to the single well and introducing water injector models. However, only the case including the injection well can describe the fluctuation in the late-time region. This spike could be the result of the considerable reduction in the injection rate after the start of the third PBU and close to the time of the fluctuation. This shows that there is hydraulic communication between the well B and the injection well D.

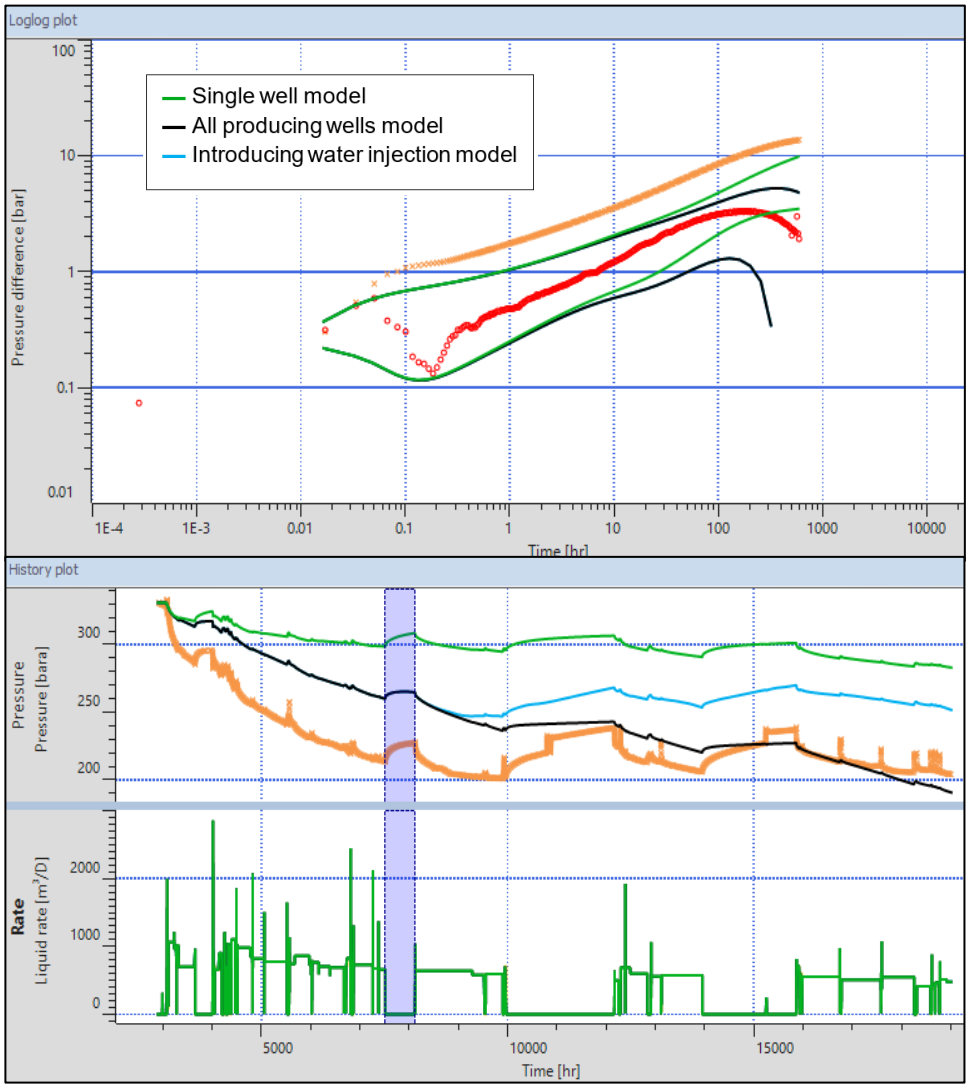

Figure 26. Analytical model results for single well case, all production wells and introducing water injection well case for well B, second PBU. Derivative plot (top) and history plot (bottom).

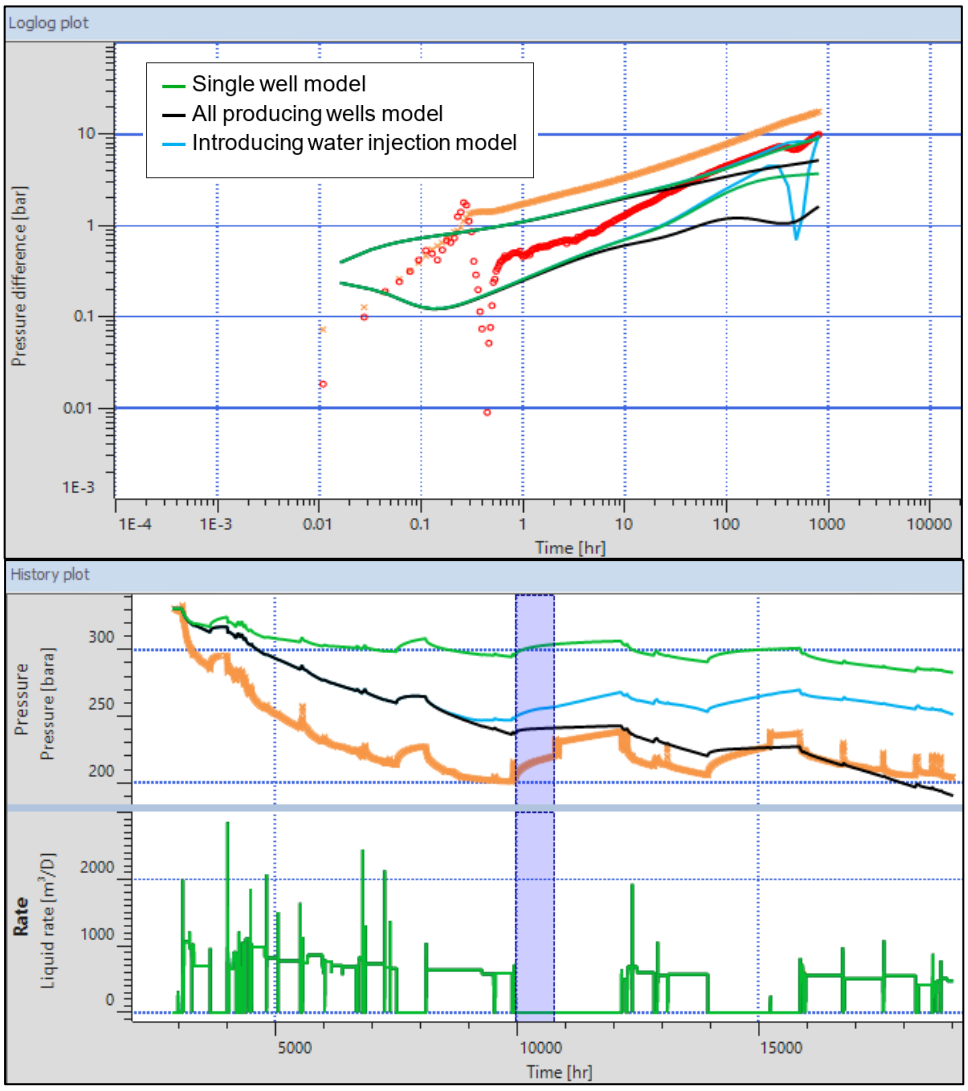

Figure 27. Analytical model results for single well case, all production wells and introducing water injection well case for well B, third PBU. Derivative (top) and history plot (bottom).

- **Fourth PBU – Well B**

In the fourth PBU for the well B, the three production wells were producing before the shut-in and all three were shut-in concurrently. Water injection in the field has already started before the fourth PBU. The analytical results considering the single well model, only production wells model, and the case including producers and injector are observed in the Figure 28. Analytical model results for single well case, all production wells and introducing water injection well case for well B, fourth PBU. Derivative (top) and history plot (bottom). The modeled derivatives are shifted down suggesting that the well B could have lower effective well length or a lower flow capacity reservoir zone compared to the values from the reference model as in the previous PBUs.

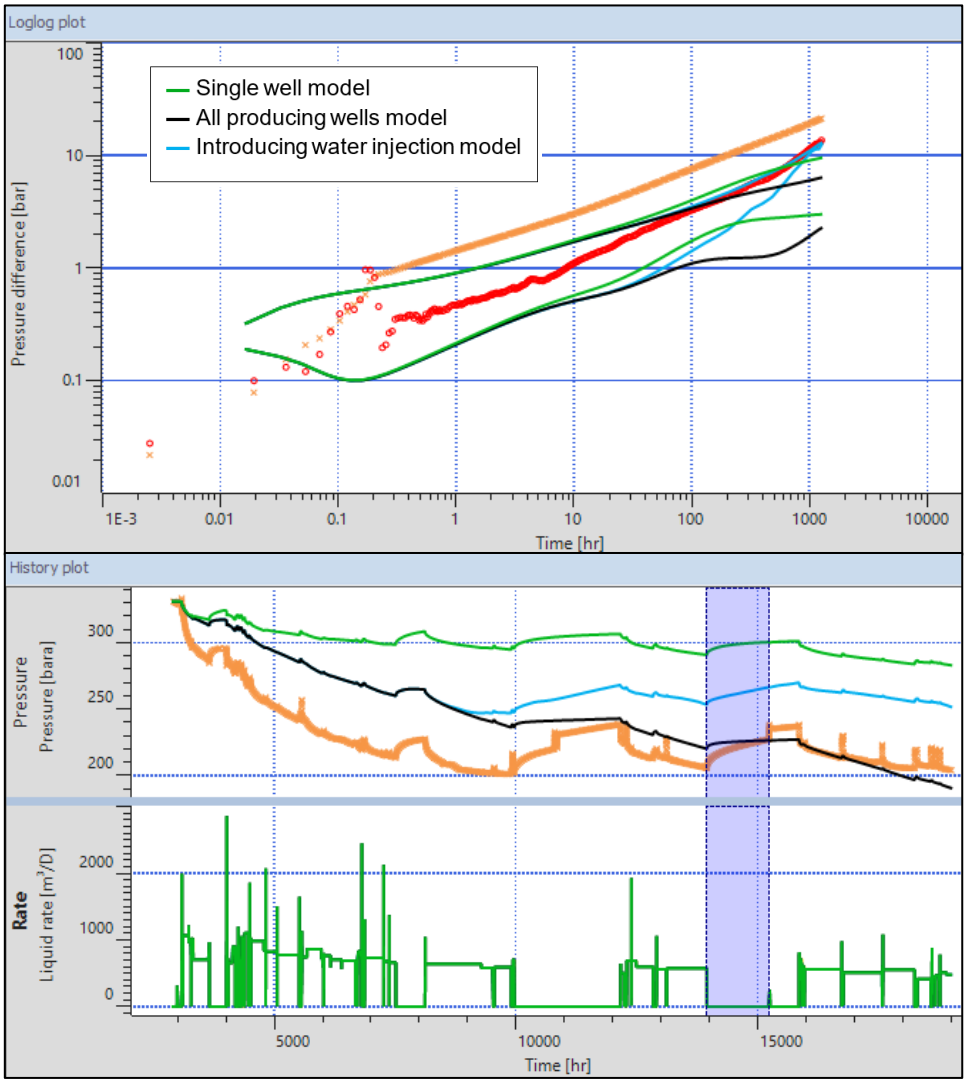

Figure 28. Analytical model results for single well case, all production wells and introducing water injection well case for well B, fourth PBU. Derivative (top) and history plot (bottom).

The model that gets closer to the observed pressure derivative is the model that introduces the water injector and producers in comparison with the single well model and the model considering only producers that do not describe the behavior of the derivative.

5.6 Well C

The well C started production in the field at about the same time as well A and before the well B. The well is located at the south east of the south compartment. Water injection starts approximately 8000 hours after the field starts producing. Four suitable pressure buildups for analysis are obtained from the data from the PDGs. For the first PBU all the three wells are producing and are shut-in for 13 days approximately, no water injection at that time. The second PBU corresponds to the interference test, where the well C (observation well) is shut-in and the nearby wells are kept producing at a constant rate. During the third and fourth PBU, all the production wells, A, B and C, are shut-in, and the water injection well, D, has been injecting for several months.

The Figure 29. Time-lapse log-log plot (top) and history plot (bottom) for well C. shows the time-lapse pressure derivatives for well C. The vertical radial flow regime, common in horizontal wells, is not seen in any of the pressure buildup periods. The pressure derivatives for the first and second PBU exhibit different behavior at the middle-time region with respect to the later PBUs. The third and fourth PBU derivatives exhibit similar behavior as both are shifted down slightly compared to the first and second PBU. The third and fourth PBUs show large effects of phase redistribution (gas and oil) in the early-time region as a result of lower pressures than the bubble point pressure at the gauges and possibly in the reservoir. No late pseudo-radial flow regime appearing in the derivatives as the transient is affected by the interference with the wells nearby and/or boundaries encountered before developing the regime.

- **First PBU – Well C**

In the first PBU for the well C, the three production wells were producing before the shut-in and all three were shut-in concurrently. No water injection in the field at the time of the first PBU. The analytical results considering the single well model, only production wells model, and the case including producers and injector are observed in the Figure 30. Analytical model results for single well case, all production wells and introducing water injection well case for well C, first PBU. Derivative (top) and history plot (bottom). The modeled derivatives adjust slightly using the reference model for the reservoir properties and distance to boundaries.

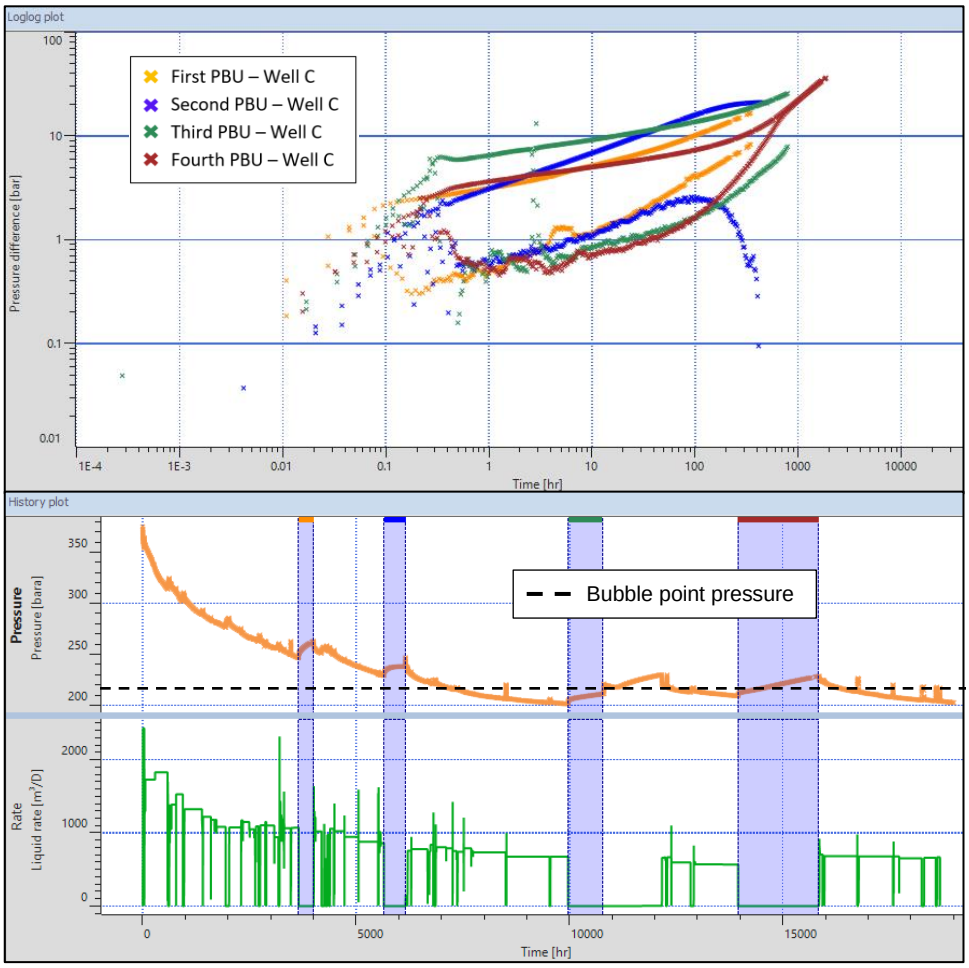

Figure 29. Time-lapse log-log plot (top) and history plot (bottom) for well C.

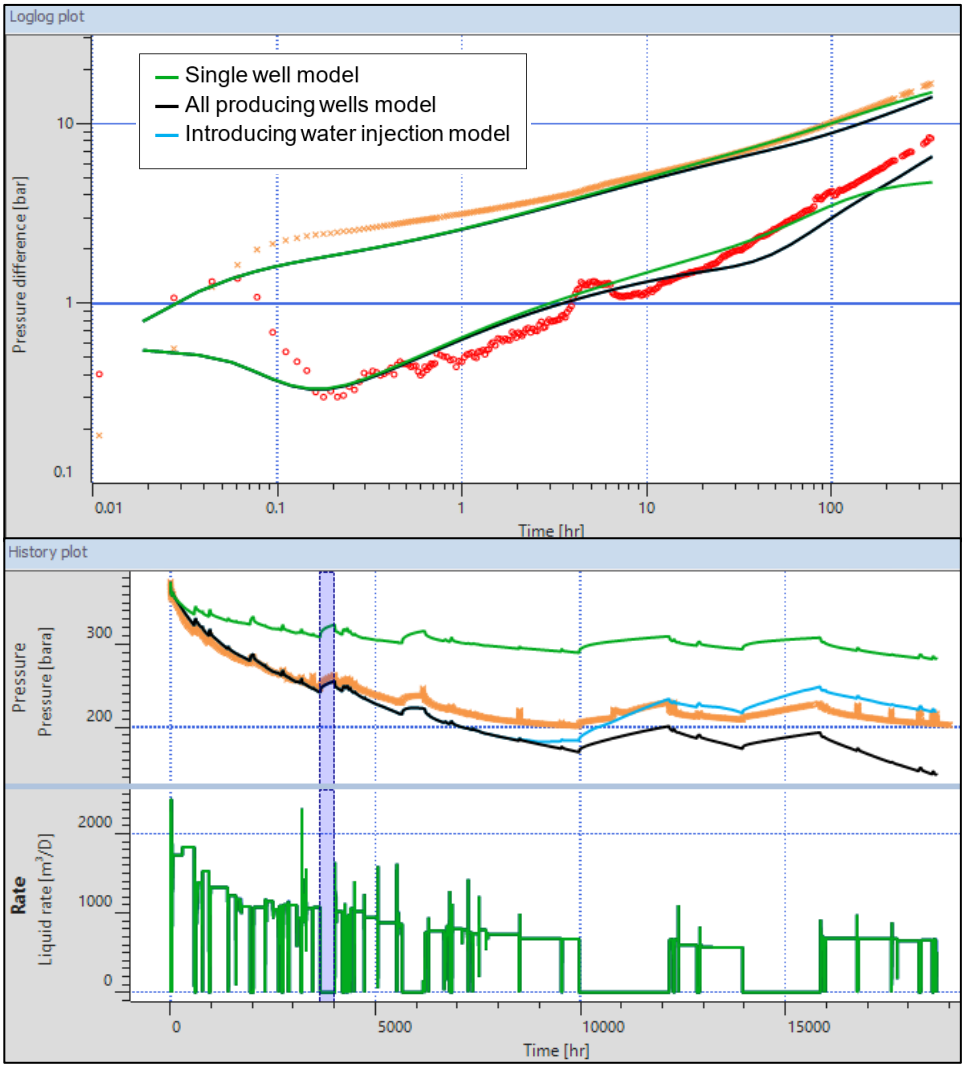

Figure 30. Analytical model results for single well case, all production wells and introducing water injection well case for well C, first PBU. Derivative (top) and history plot (bottom).

The single well model does not describe the behavior of the derivative at late-time region in comparison to the cases considering the producing wells. This shows that there could be hydraulic communication between the producers. The model introducing water injection only affects the history plot and it can be observed that it supports pressure and reduces the pressure declination as it is observed in the field.

The sensitivity to effective well length based on estimated values from the PLT results is shown in the Figure 31. Sensitivity to effective well length for well C based on PLT. Derivative plot (top) and history plot (bottom). The reference model has a low value compared to the drilled horizontal section. The three cases considered where generated using all producer and injector model. The plot shows that an increased effective well length shifts down the modeled derivative; however, in this case the range of estimated values that can be encountered is narrower compared to the other wells.

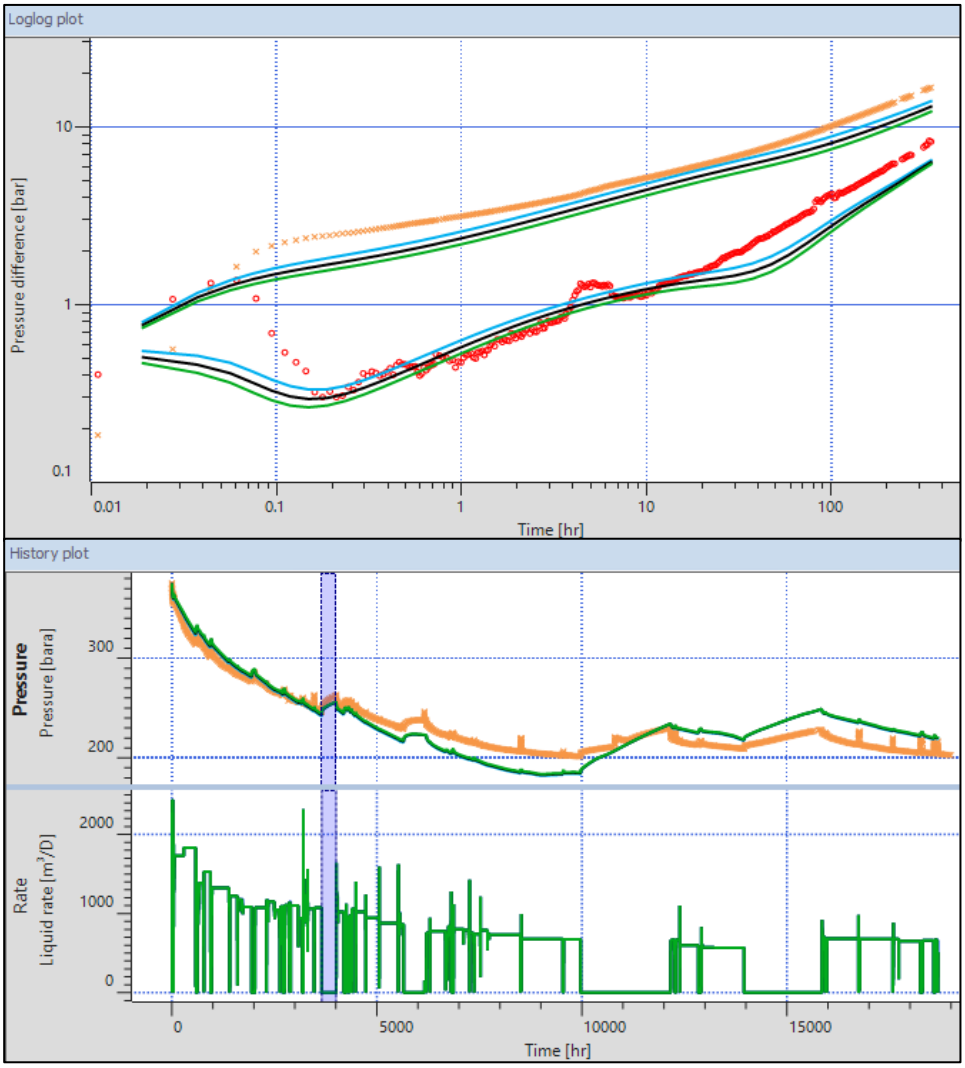

Figure 31. Sensitivity to effective well length for well C based on PLT. Derivative plot (top) and history plot (bottom).

- **Second PBU – Well C**

The second PBU for the well C corresponds to the interference test. The producing wells nearby, A and B, were producing along with well C before the shut-in of well C (observation well); however, well A and B (active wells) keep producing during the PBU of C. No water injection in the field at the time of the second PBU. The analytical results considering the single well model, only production wells model, and the case including producers and injector are observed in the Figure 32. Analytical model results for single well case, all production wells and introducing water injection well case for well C, second PBU. Derivative plot (top) and history plot (bottom).

The single well model does not describe the behavior of the derivative at late-time region in comparison to the cases considering the producing wells. This suggests that there is hydraulic communication between the producers. The model introducing water injection only affects the history plot and it can be observed that it supports pressure and reduces the pressure declination as observed in the field.

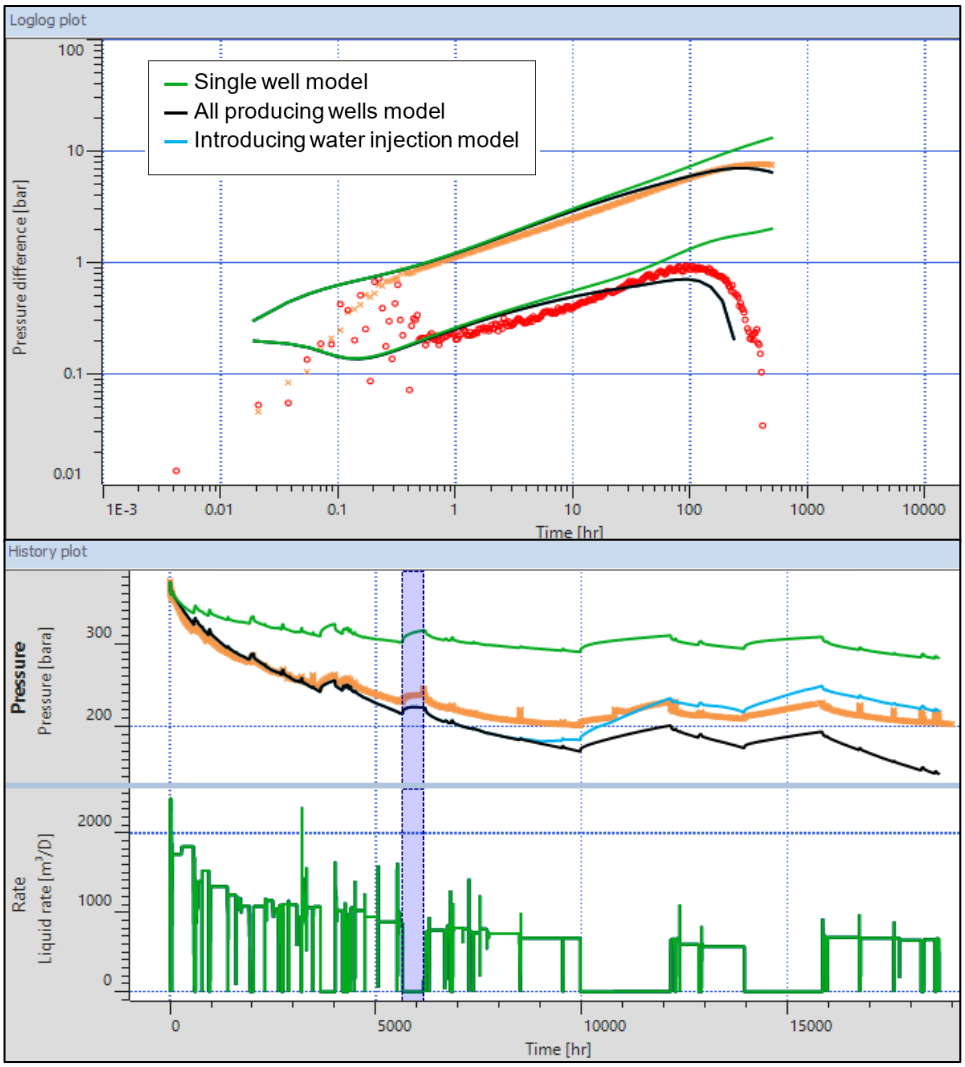

Figure 32. Analytical model results for single well case, all production wells and introducing water injection well case for well C, second PBU. Derivative plot (top) and history plot (bottom).

- **Third PBU – Well C**

In the third PBU for the well C, the three production wells were producing before the shut-in and all three were shut-in concurrently. Water injection in the field has already started before the third PBU. The analytical results considering the single well model, only production wells model, and the case including producers and injector are observed in the Figure 33. Analytical model results for single well case, all production wells and introducing water injection well case for well C, third PBU. Derivative (top) and history plot (bottom). The modeled derivatives are shifted up suggesting that the well C could have experienced an increase in effective well length or contribution of an underlying formation that increases the kh compared to the previous PBU. This is the same behavior as experienced in the well A.

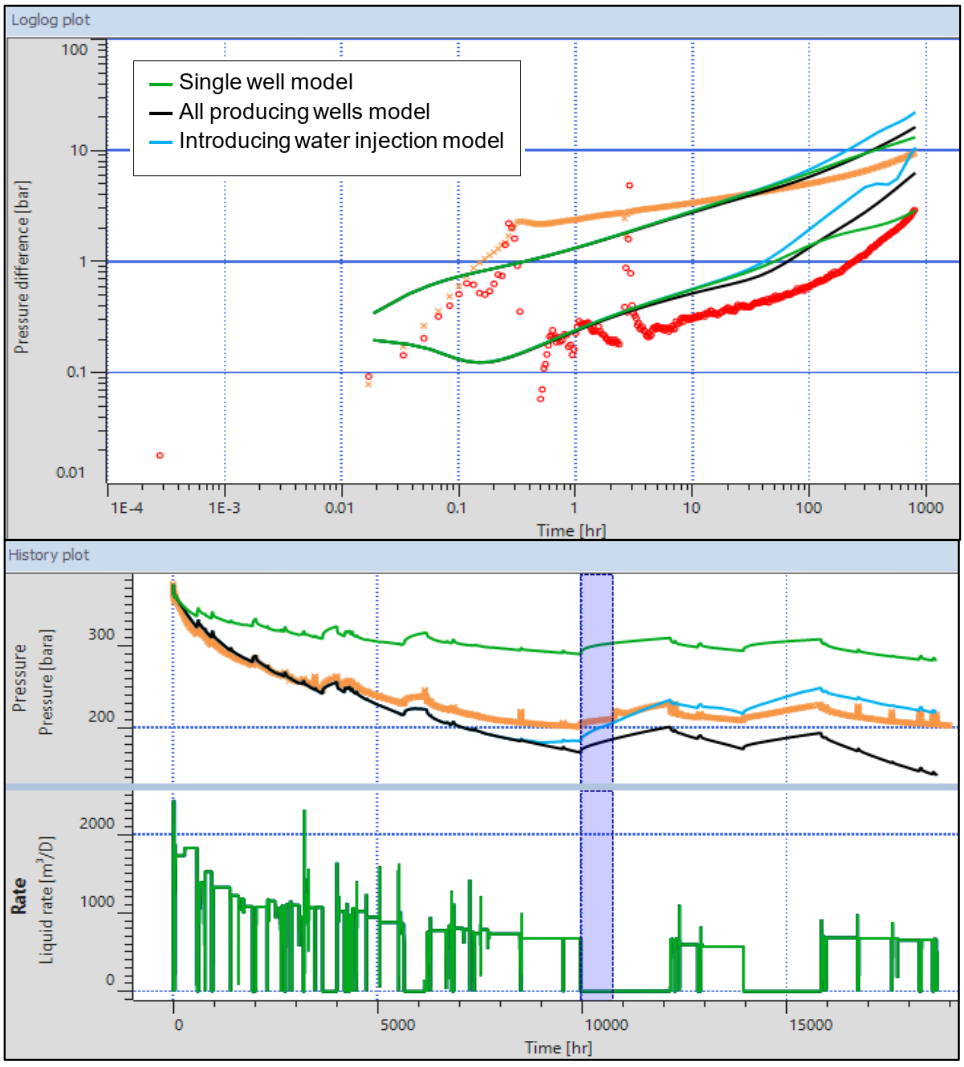

Figure 33. Analytical model results for single well case, all production wells and introducing water injection well case for well C, third PBU. Derivative (top) and history plot (bottom).

The all producing wells model and the model introducing water injection show similar and closer behavior to the observed derivative in the late-time region in comparison to the single well model. A fluctuation like the one noticed in the well B in the same PBU and resulting because of the considerable reduction in the injection rate is modeled but it is not observed in the pressure response. As a result of this, all producing wells model could describe better the derivative. However, considering only the producing wells do not match the pressure observed pressure support shown in the history plot. This could indicate that there is poor communication between the producing well C and the injection well D.

Increasing effective well length model, well C and third PBU.

A possible reason of the shifting down of the derivative after water injection could be an increase in the effective well length from 1355 m. However, to get a closer match of the pressure derivative it is required am increase of this parameter to 2500 m, the log-log plot reflecting this change is shown in the Figure 34. Increased effective well length to 2500 m for well C and third PBU. If we consider that the drilled horizontal section for this well is 1600 m, and an increase in 900 m could not be used based on the data obtained, then it is possible that is the result of an increase in the flow capacity of the reservoir due to an increase in the permeability or the additional thickness contributing.

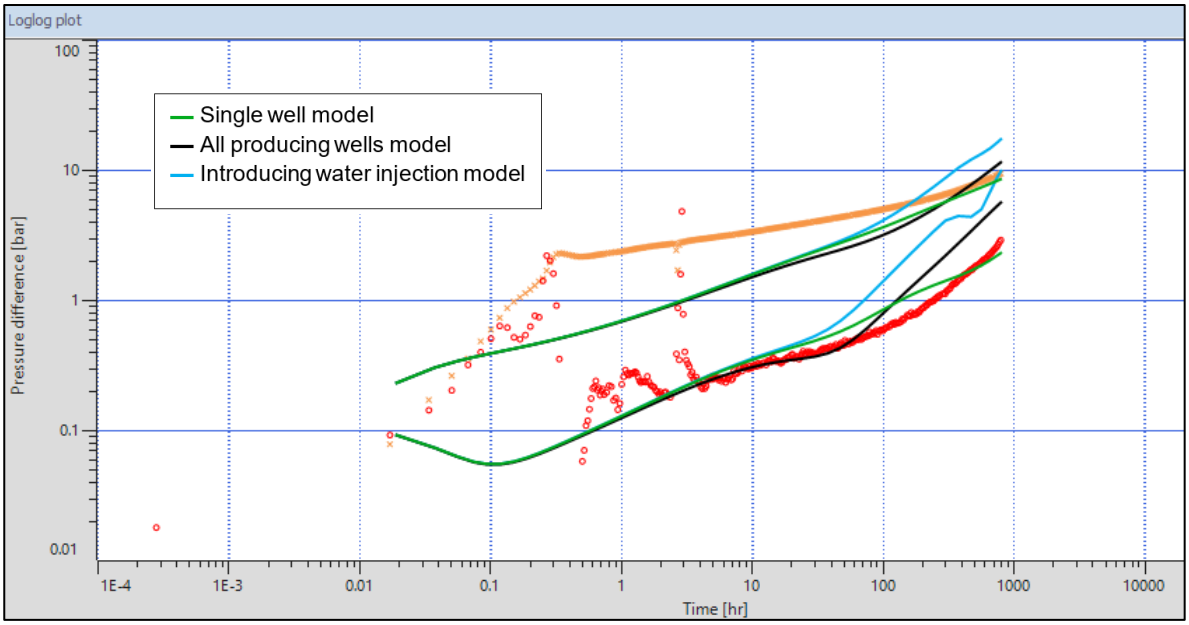

Figure 34. Increased effective well length to 2500 m for well C and third PBU.

- **Fourth PBU – Well C**

In the fourth PBU for the well C, the three production wells were producing before the shut-in and all three were shut-in concurrently. Water injection in the field has already started before the fourth PBU. The analytical results considering the single well model, only

production wells model, and the case including producers and injector are observed in the Figure 35. Analytical model results for single well case, all production wells and introducing water injection well case for well C, fourth PBU. Derivative plot (top) and history plot (bottom). The modeled derivatives are shifted up suggesting that the well C could have experienced an increase in effective well length or contribution of an underlying formation that increases the kh compared to the previous PBU.

The model with all producing wells and the model introducing water injection show similar and closer behavior to the observed derivative in the late-time region in comparison to the single well model. Nonetheless, the model that gets closer to the observed pressure derivative is the model that introduces the water injector and producers. This model also accounts for the pressure support observed in the history plot.

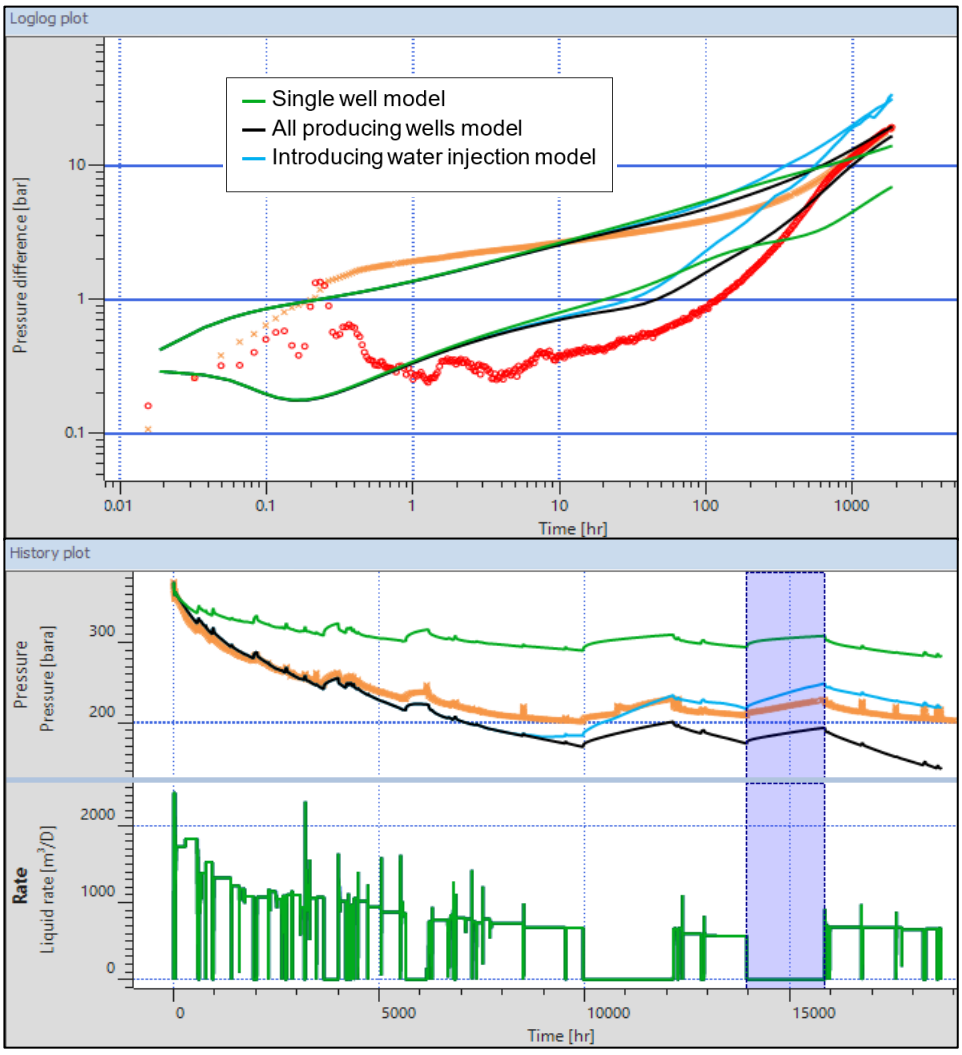

Figure 35. Analytical model results for single well case, all production wells and introducing water injection well case for well C, fourth PBU. Derivative plot (top) and history plot (bottom).

To illustrate the observations mentioned previously from time-lapse PTA regarding the different behavior in the pressure derivatives after water injection starts in the field for the wells in the southern part, a map of the oil field is shown in the Figure 36. Map of the field and time-lase PTA of the producing horizontal wells. with the time-lapse PTA for each production well.

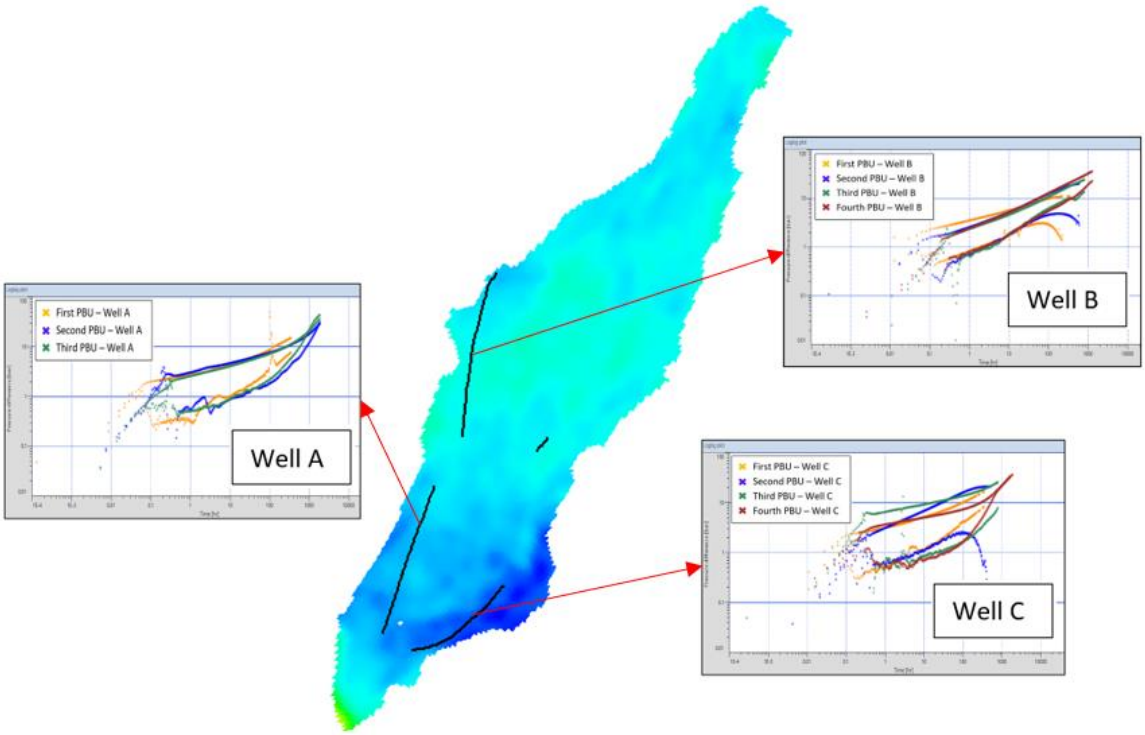

Figure 36. Map of the field and time-lase PTA of the producing horizontal wells.

6. Numerical model: Interpretation and simulation results

Once the analytical modelling was carried out, the values of the reservoir parameters obtained from this is used in the numerical model part. As observed from the analytical results, some of the mismatches between the modeled derivative and the pressure response derivative could be explained by an increase in the effective well length with the respect to the values from the PLT data results. Therefore, to establish if this parameter could explain by itself the difference in the derivatives, the drilled horizontal section well lengths are used in the numerical modelling.

The real geometry of the field for the analytical model set-up, shown in Figure 12. Sketch of the field and approximated shape (rectangle) of closed system., and established from seismic interpretation was used for the numerical model as it is observed in the Figure 37. 2D geometry plot used in numerical model and estimated boundaries from geological map., the model uses voronoi grids and includes all the wells in the southern compartment with the reservoir properties from the reference model.

6.1 Numerical model set-up

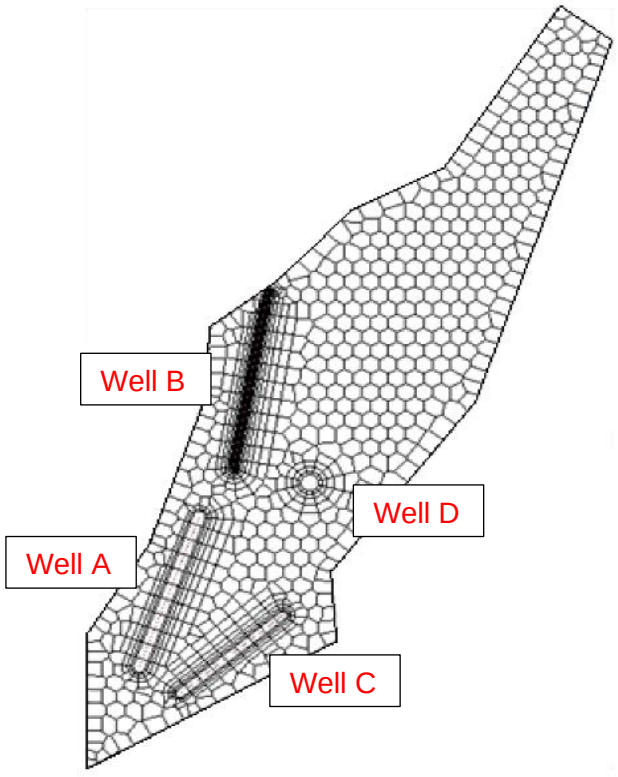

Figure 37. 2D geometry plot used in numerical model and estimated boundaries from geological map.

6.2 Well A

- **First PBU – Well A**

The results with the numerical model using the drilled horizontal section well lengths are observed in the Figure 38. Numerical model results for well A, first PBU. Derivative plot (top) and history plot (bottom). for well A and first PBU, no water injection in the field at the time of this test. Better match of the pressure difference and pressure derivative compared to the analytical results observed in the log-log plot. However, good description of the major well interference features from the analytical models is observed. The reservoir parameters values used seem to describe the flow behavior of the formation studied. The effective well lengths match better with longer effective well lengths compared to the chemical PLT data.

From the log-log plot, the late-time region section of the curve from the model follows the same trend as the observed pressure derivative, confirming the interference with the producing wells nearby. The history plot simulated describes the connected volumes observed for the period considered.

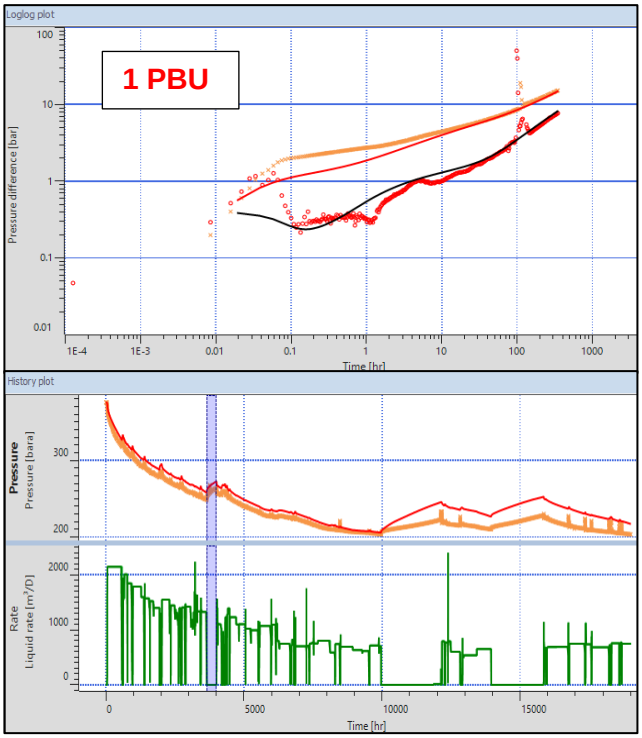

Figure 38. Numerical model results for well A, first PBU. Derivative plot (top) and history plot (bottom).

- **Second PBU – Well A**

The results using the numerical model for the well A and 2 PBU after water injection has started in the field is shown in the Figure 39. Numerical model results for well A, second PBU. Derivative plot (top) and history plot (bottom). The significant reduction in the water injection rate of the injector during this period, as discussed in the well B, is modeled in the pressure derivative after 300 hr. of shut-in as a reduced slope in the curve, similar behavior in the observed derivative. This same trend indicates communication between the production and injection well.

Despite the confirmation of the reservoir connectivity between the producer and injector, the modeled derivative is shifted up with respect to the observed derivative, indicating a possible increase in kh after water injection as mentioned in the analytical results. This could be explained by the activation of additional layers that were not contributing or flowing but once the water injection took place, they started to move towards the production well. The model shows a more optimistic pressure support than the one observed in the history plot.

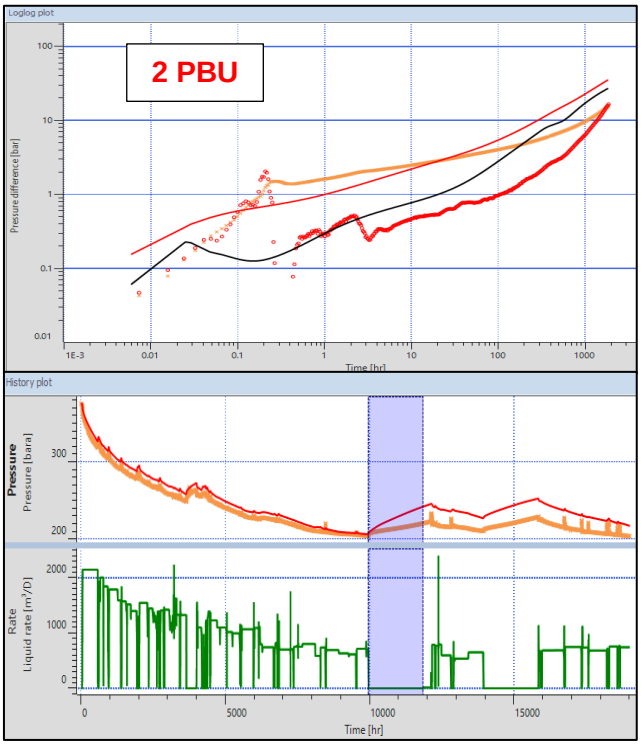

Figure 39. Numerical model results for well A, second PBU. Derivative plot (top) and history plot (bottom).

- **Third PBU – Well A**

Similarly to the previous PBU, the numerical model results for well A and 3 PBU after water injection in the field has started, shown in the Figure 40. Numerical model results for well A, third PBU. Derivative plot (top) and history plot (bottom). suggest that the flow capacity of the reservoir around the well has increased as a result of injecting water nearby. In the history plot, the model shows a more optimistic pressure support than the one observed from pressure response.

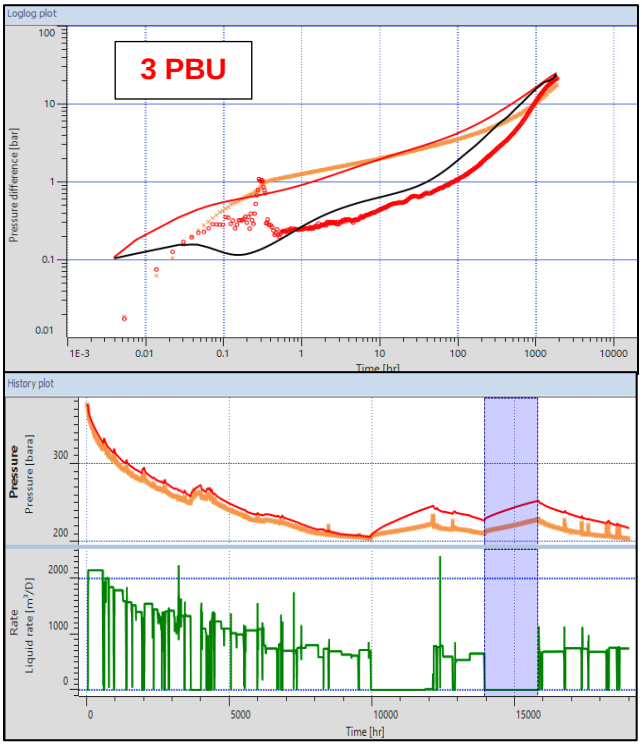

Figure 40. Numerical model results for well A, third PBU. Derivative plot (top) and history plot (bottom).

6.3 Matching numerical model of well B

The results with the numerical model using the drilled horizontal section well lengths for well B are similar to the analytical results using the same reservoir parameters. The third PBU showed a small difference in the amplitude of the fluctuation generated by the pulse given by the reduction in the injection rate after the shut-in in the production wells, as discussed previously. This indicates a good description of the major well interference features from the analytical models.

The log-log plot for all the PBUs of well B, suggests that the shifting down of the modeled derivative with respect to the observed derivative is due to location of the well at a low flow capacity area of the reservoir. According to the chemical PLT results, a reduced effective well length cannot explain such change.

The match obtained for the well B started with the 3 PBU, where the interference with the injector well is clearly defined. The mentioned fluctuation amplitude depends on the flow capacity, mainly permeability and to represent the connected volumes correctly, a reduced value in thickness is required. Using the numerical model, the values of the reservoir properties for the well B that get the best match is a permeability of 30 md and a thickness of 10 m.

The numerical model results using the parameters from the reference model, that matched the southern parallel wells, and the reduced flow reservoir capacity model that match the pressure response for well B are compared in the Figure 41. Log-log plot of first PBU for well B, reference model (top left) and match (top right) derivative, and second PBU, reference model (bottom left) and match (bottom right) derivative. PBUs before water injection in the field. and Figure 42. Log-log plot of third PBU for well B, reference model (top left) and match (top right) derivative, and fourth PBU, reference model (bottom left) and match (bottom right) derivative. PBUs before water injection in the field., for the PBUs before and after water injection, respectively.

As a result of this better match, the reduced flow capacity around the well B, could be explained by a reduction in the reservoir quality (permeability of 30 md and thickness of 10 m). The 1 PBU deviates slightly, probably due to a small reduction in the effective well length after the cleanup, that then increases for the following PBUs.

The pressure response simulated for the well B, shown in the Figure 43. History plot of well B and simulated response for the reference model (top) and match model (bottom)., indicates that the match model adequately describes the connected volumes and the pressure support as shown in the history plot.

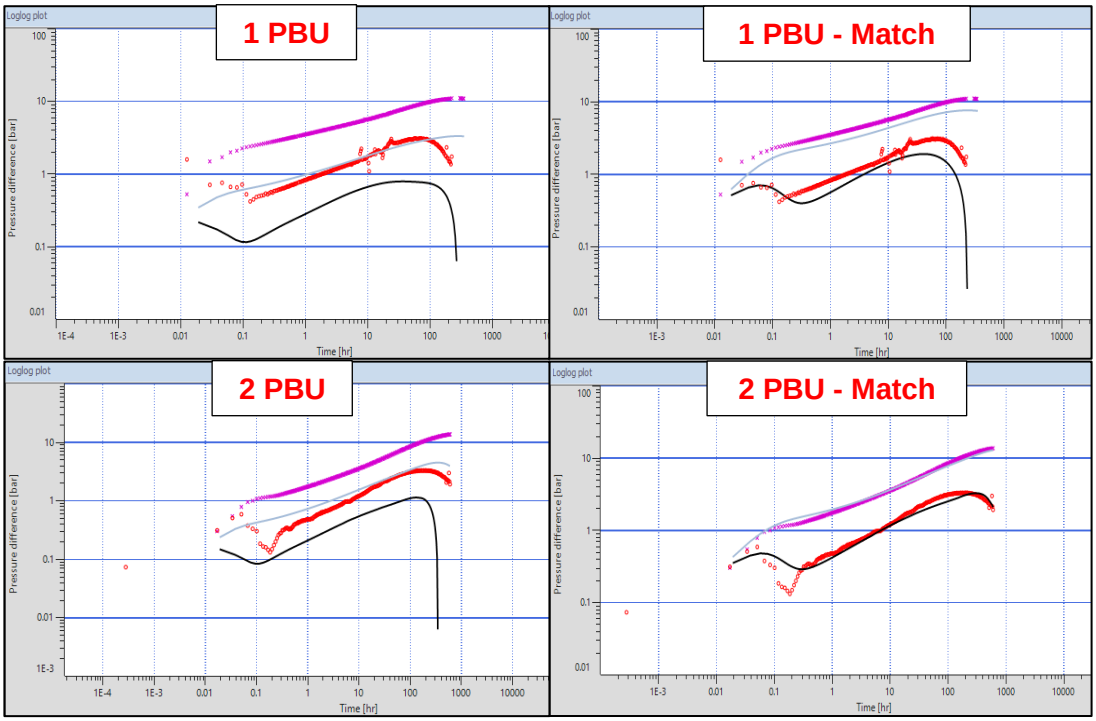

Figure 41. Log-log plot of first PBU for well B, reference model (top left) and match (top right) derivative, and second PBU, reference model (bottom left) and match (bottom right) derivative. PBUs before water injection in the field.

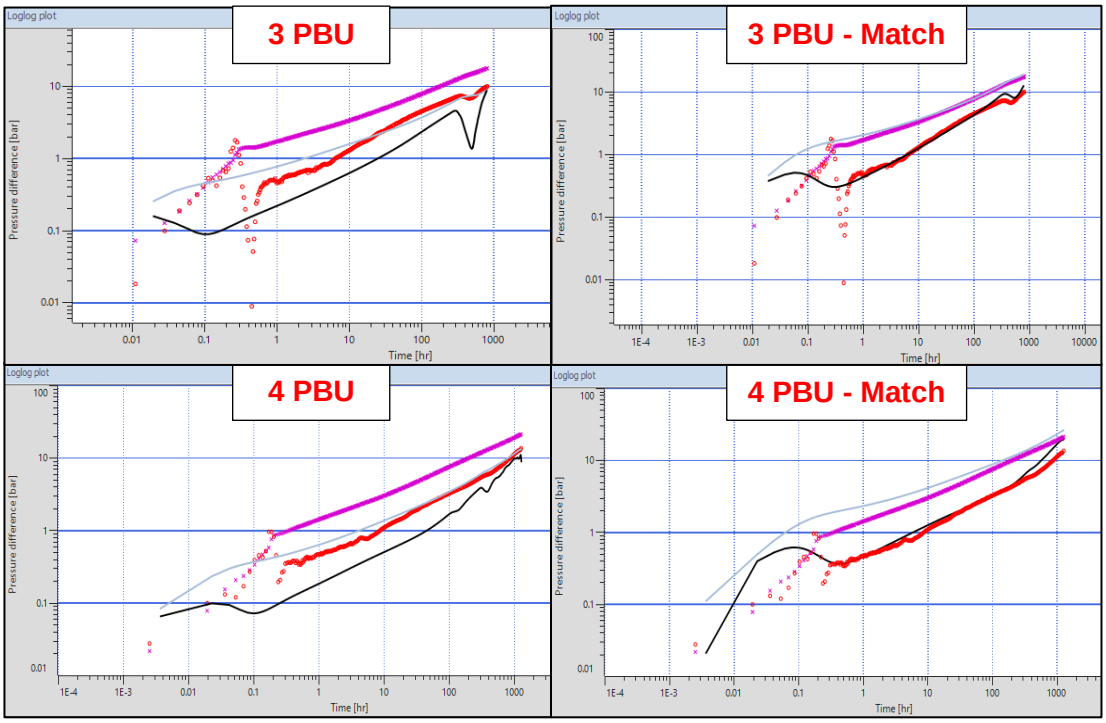

Figure 42. Log-log plot of third PBU for well B, reference model (top left) and match (top right) derivative, and fourth PBU, reference model (bottom left) and match (bottom right) derivative. PBUs before water injection in the field.

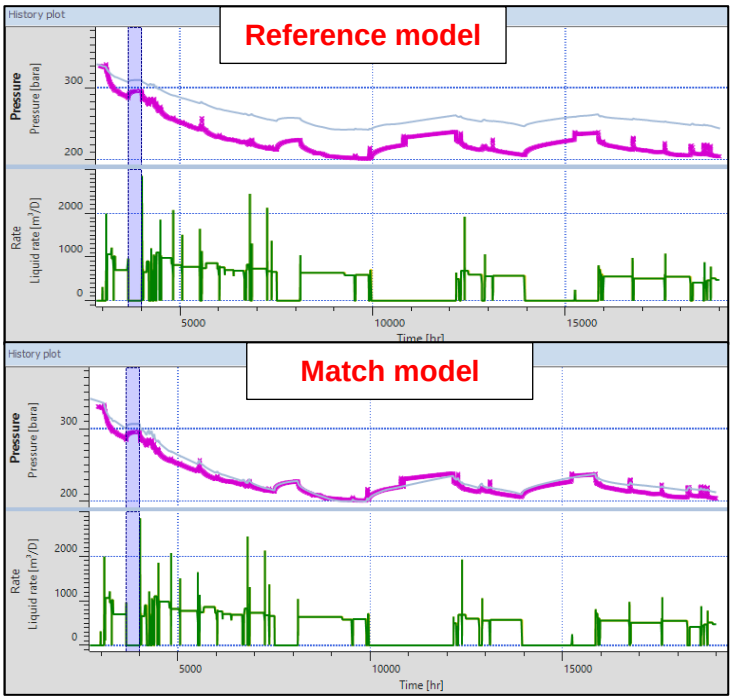

Figure 43. History plot of well B and simulated response for the reference model (top) and match model (bottom).

6.4 Well C

- **First PBU – Well C**

The results with the numerical model using the drilled horizontal section well lengths are observed in the Figure 44. Numerical model results for well C, first PBU. Derivative plot (top) and history plot (bottom). for well C and first PBU, no water injection in the field at the time of this test. Better match of the pressure difference and pressure derivative compared to the analytical results observed in the log-log plot. However, good description of the major well interference features from the analytical models is observed. The reservoir parameters values used seem to describe the flow behavior of the formation studied. These values are the same as for the well A that is parallel to well C in the southern part; therefore, the area between these wells could be described using this reservoir properties. The effective well lengths match better with longer effective well lengths compared to the chemical PLT data.

From the log-log plot, the late-time region section of the curve from the model follows the same trend as the observed pressure derivative, confirming the interference with the producing wells nearby. The history plot simulated describes the connected volumes observed for the period considered.

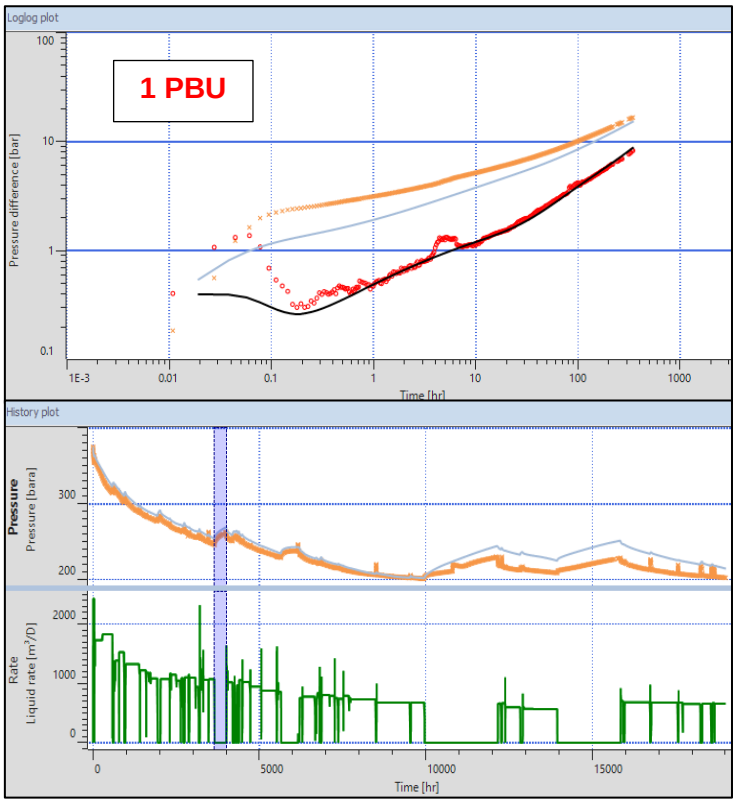

Figure 44. Numerical model results for well C, first PBU. Derivative plot (top) and history plot (bottom).

- **Second PBU – Well C**

Similarly to the 1 PBU, the log-log plot with the numerical model using the drilled horizontal section, shown in the Figure 45. Numerical model results for well C, second PBU. Derivative plot (top) and history plot (bottom). for well C and second PBU (no water injection in the field for this period), obtains a better match of the pressure derivatives than the analytical results applying the reservoir parameters set in the reference model for the numerical model.

From the log-log plot, the late-time region section of the curve from the model follows the same trend as the observed pressure derivative, both curves are going down as a result of the interference with other producing wells nearby. This period corresponds to the interference test, being well C the observation well, and well A and B the active wells and producing during this period. The history plot simulated describes the connected volumes observed for the period considered.

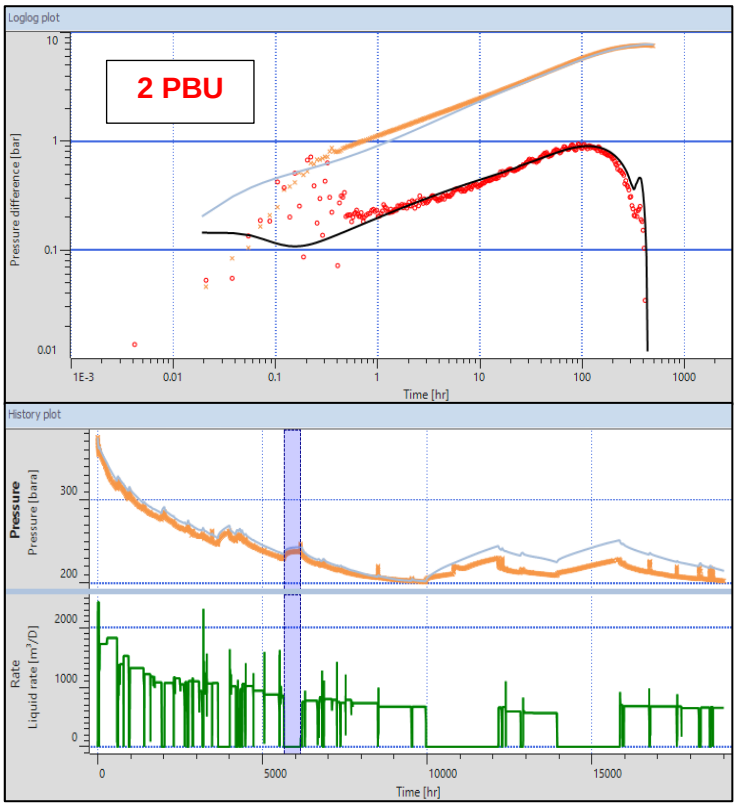

Figure 45. Numerical model results for well C, second PBU. Derivative plot (top) and history plot (bottom).

- **Third PBU – Well C**

The results using the numerical model for the well C and 3 PBU after water injection has started in the field is shown in the Figure 46. Numerical model results for well C, third PBU. Derivative plot (top) and history plot (bottom). The significant reduction in the water injection rate of the injector during this period, as discussed in the well A and B, is modeled in the pressure derivative after 300 hr. of shut-in. However, for this well the response in the model is observed later and it is not that evident in the derivative from the pressure response, as the well is further. This difference could be the result of a poorer reservoir connectivity between the well C and the injector compared to the well A and the injector. In the third PBU, the pressure possibly is below the bubble point pressure in the top of the reservoir, increasing the skin of the well C.

Despite the confirmation of the reservoir connectivity between the producer and injector, the modeled derivative is shifted up with respect to the observed derivative, indicating a possible increase in kh after water injection as mentioned in the analytical results. This could be explained by the activation of additional layers that were not contributing or flowing but once the water injection took place, they started to move towards the production well. The model

shows a more optimistic pressure support than the one from the pressure response as observed in the history plot.

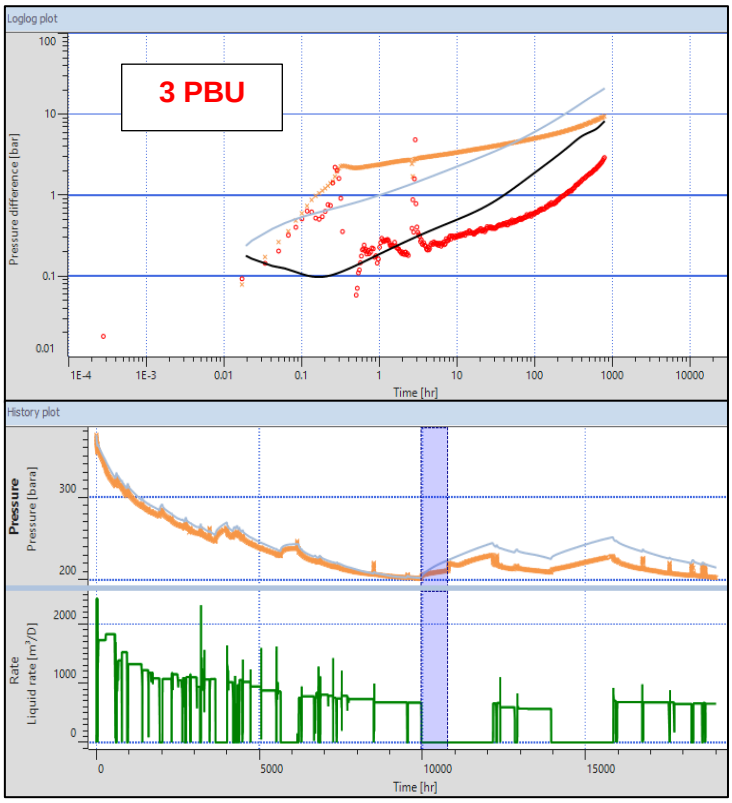

Figure 46. Numerical model results for well C, third PBU. Derivative plot (top) and history plot (bottom).

- **Fourth PBU – Well C**

Similarly to the previous PBU, the numerical model results for well C and 4 PBU after water injection in the field has started, shown in the Figure 47. Numerical model results for well C, fourth PBU. Derivative plot (top) and history plot (bottom)., suggest that the flow capacity of the reservoir around the well has increased as a result of injecting water nearby. In the history plot, the model shows a more optimistic pressure support than the one observed from pressure response.

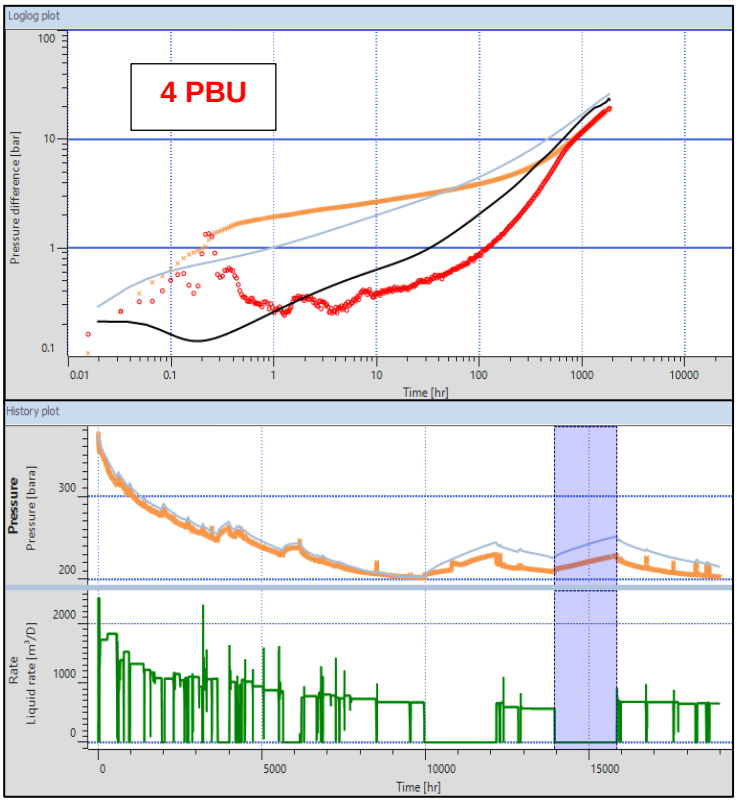

Figure 47. Numerical model results for well C, fourth PBU. Derivative plot (top) and history plot (bottom).

6.5 Sensitivity to effective well length, thickness, and permeability on well A

To study the similar behavior observed in well A and C after water injection starts in the field, a sensitivity analysis to effective well length, thickness and permeability is carried out on well A. As discussed previously, the shift down of the pressure derivative with respect to the reference model, that was describing the response adequately for the PBUs before water injection in the field, could be explained by an increased in the effective well length, or increase in the flow capacity of the reservoir, thickness and permeability product.

The increase in the effective well length could be the result of the sidetrack in the well A but not applicable in well C, as not sidetrack was done for this well. The sensitivity analysis to effective well length for well A shown in the Figure 48. Sensitivity to effective well length for PBUs after water injection started in the field for well A., indicates that it is a possible reason to consider an increase of 500 m in the effective well length; however, the match is not the most adequate to describe the change.

The sensitivity to thickness, for well A and the PBUs after water injection started in the field, is shown in the Figure 50. Sensitivity to thickness for PBUs after water injection started in

the field for well A. Increasing the thickness explains the shifting down of the curve and an increase in 8 m to the reference model thickness, to a total of 20 m, gets the better match of the pressure derivatives. By increasing the thickness, the pressure simulated in the history plot is not representative if considering the whole time; nonetheless, as the increase in thickness is observed after water injection, the simulated pressure after this occurs could match the trend of the pressure support. This increase could suggest that the water injection is moving fluid from some layers that were inactive before the injector was opened, this behavior is only observed in the southern part of the field.

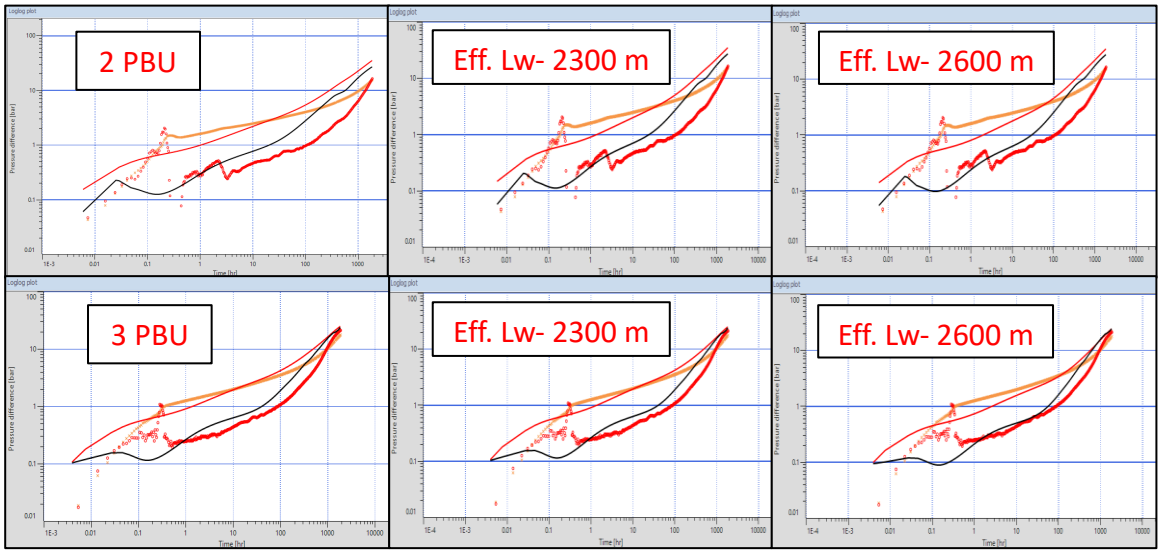

Figure 48. Sensitivity to effective well length for PBUs after water injection started in the field for well A.

The sensitivity to permeability for the same well and PBUs is observed in the Figure 49. Sensitivity to permeability for PBUs after water injection started in the field for well A., values around 120 md gives an adequate match, not as good as the thickness match, but it describes the shifting down of the derivatives. The simulated pressures increase as with the thickness, but to a lower degree.

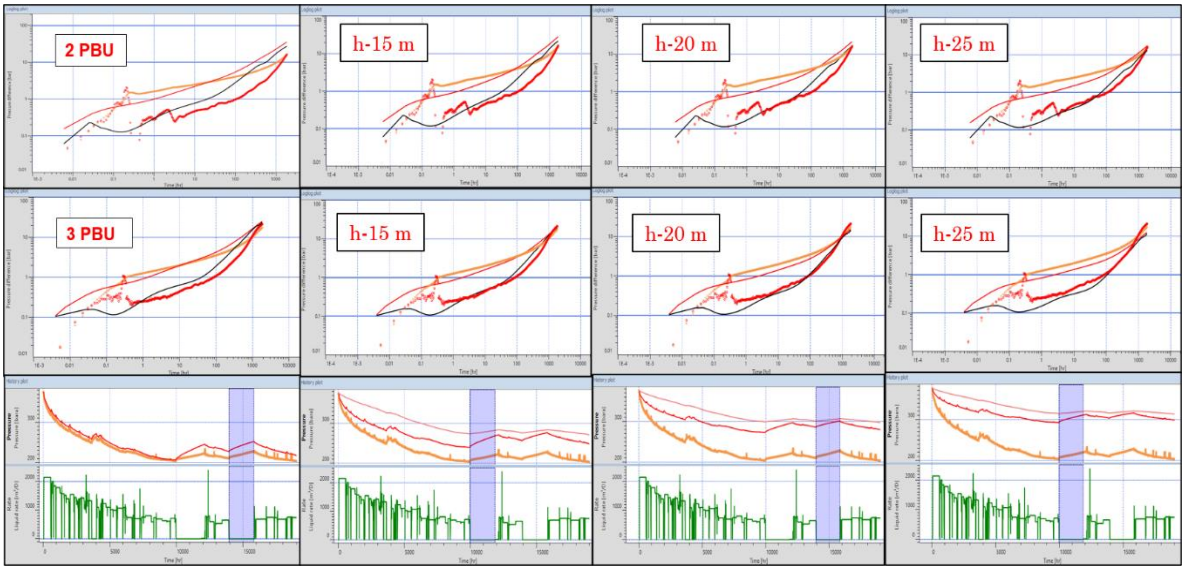

Figure 50. Sensitivity to thickness for PBUs after water injection started in the field for well A.

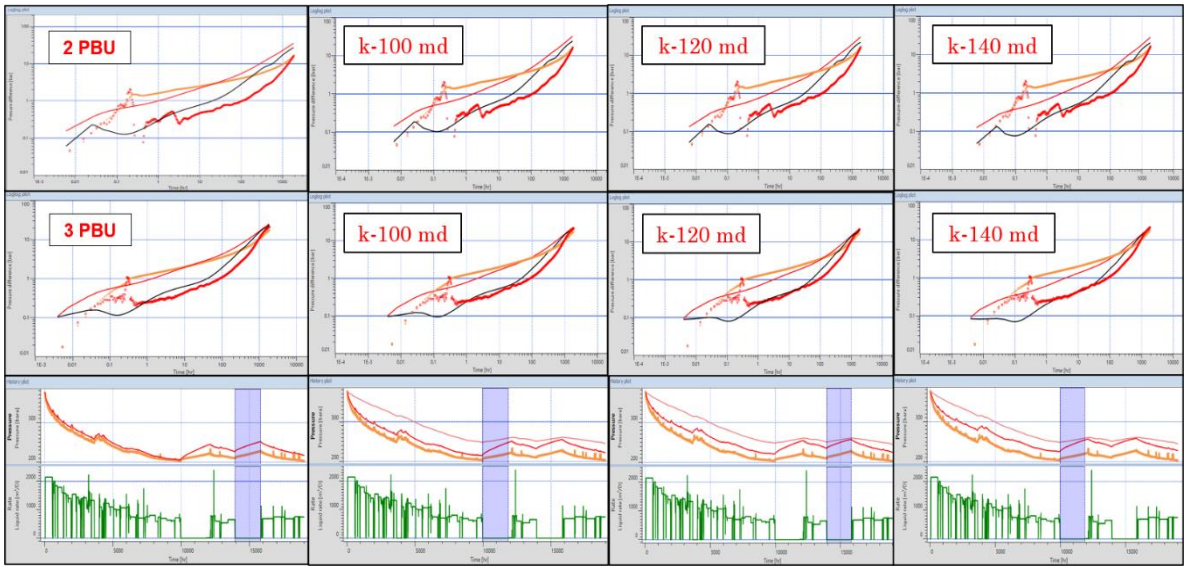

Figure 49. Sensitivity to permeability for PBUs after water injection started in the field for well A.

6.6 Multi-layer numerical model analysis

A 3D full field numerical analysis is carried out including all the wells in the southern part of the field, well A, B, C, and the injector D, as it is shown in the Figure 51. 3D geometry plot for multilayer model. The bottom layer considered in this model may be explained by the lower quality of the reservoir at the bottom of the main layer separated by thin shale layers, limiting the crossflow and presenting a low transmissibility between the two flow units. This study is carried out to analyze the shifting down effect of the pressure derivatives after water injection has started in the field.

The reservoir properties of the bottom layer are the same as the upper layer, considered in the 2D model, but the thickness is lower and selected from the geology model as an average, with a value of 7 m. Three cases with different transmissibility values between the layers are considered, the first with a value of 1, the second with a value of 0.1 and the third with a value of 0.01.

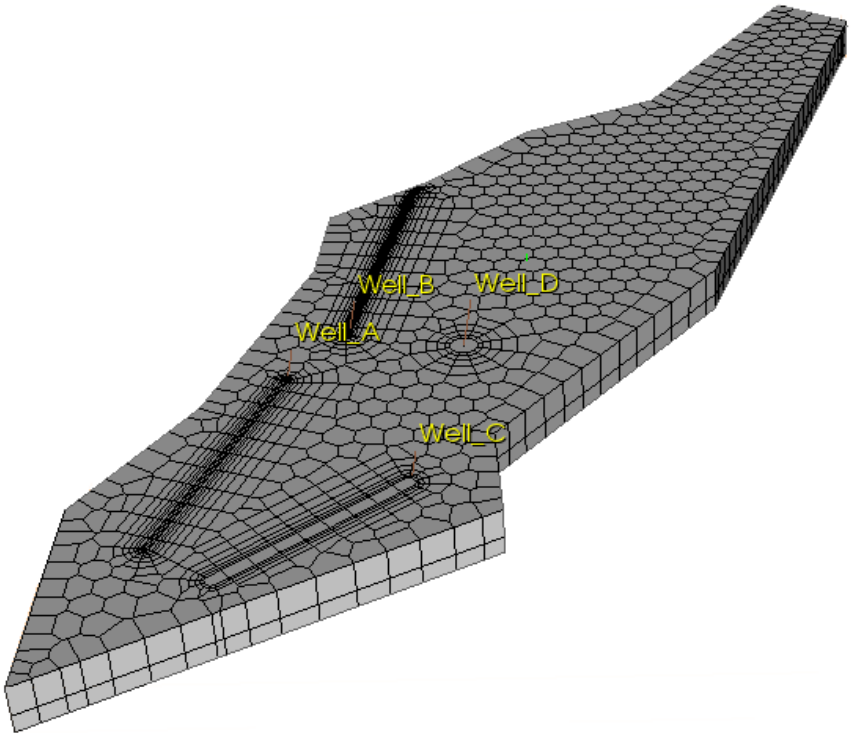

Figure 51. 3D geometry plot for multilayer model. Upper layer (main reservoir) and bottom layer displayed.

The Figure 52. Multilayer model log-log plot and history plot after water injection started in the field for well A (left) and well C (right). Transmissibility between layers equal to 1. shows

the numerical results for the multilayer model with a transmissibility of 1. As observed from the log-log plots for the pressure derivatives after water injection started in the field, the match is better for well A and C, and consistent with the sensitivity analysis results for the numerical results. These wells are the ones that change its behavior after water injection starts. The well B, as mentioned before, is matched with a low kh value for the reservoir around this well; therefore, it is not considered in the multilayer analysis.

Considering that the transmissibility between the bottom and upper layer is low, the value is reduced and the results of log-log plots for well A and C for a transmissibility of 0.1 and 0.01 are shown in the Figure 53. Multilayer model log-log plot and history plot after water injection started in the field for well A (left), and well C (right). Transmissibility between layers equal to 0.1. and Figure 54. Multilayer model log-log plot and history plot after water injection started in the field for well A (left), and well C (right). Transmissibility between layers equal to 0.01., respectively. From these results, a value around 0.1 matches better the pressure response observed in the derivatives for well A and C after the water injection behavior. A more appropriate description of the early and middle-time region is obtained for this transmissibility value with respect to 1 and 0.01.

The difference in the connected volumes from the observations and simulated model for the multilayer option is better than the single layer model, as less optimal pressure support is considered, matching the pressure response, this if it is considered that the contribution of the additional layer starts after water injection; in other words, before water injection, less fluid was being moved towards the well A and C, and once the water injection started, the inactive fluid in adjacent layers (that can be within the same main layer or in an underlaying layer) became active. Therefore, before water injection started in the field, the simulated pressure for well A and C that describes the pressure response is the one from the 2D model with a thickness of 12 m, and after water injection, the increase in thickness describes the pressure support observed for these wells.

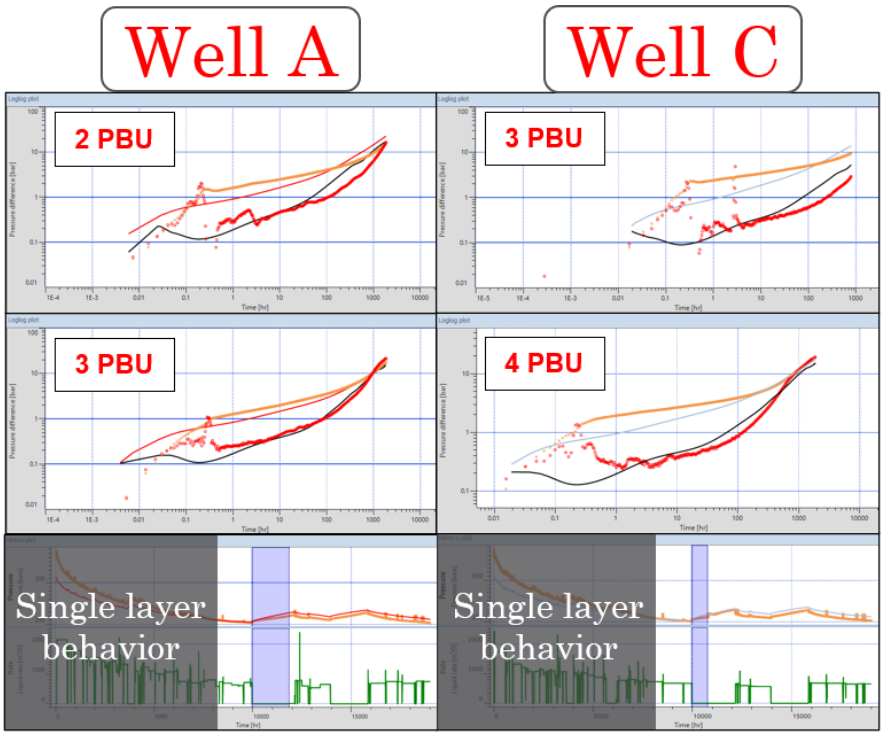

Figure 52. Multilayer model log-log plot and history plot after water injection started in the field for well A (left) and well C (right). Transmissibility between layers equal to 1.

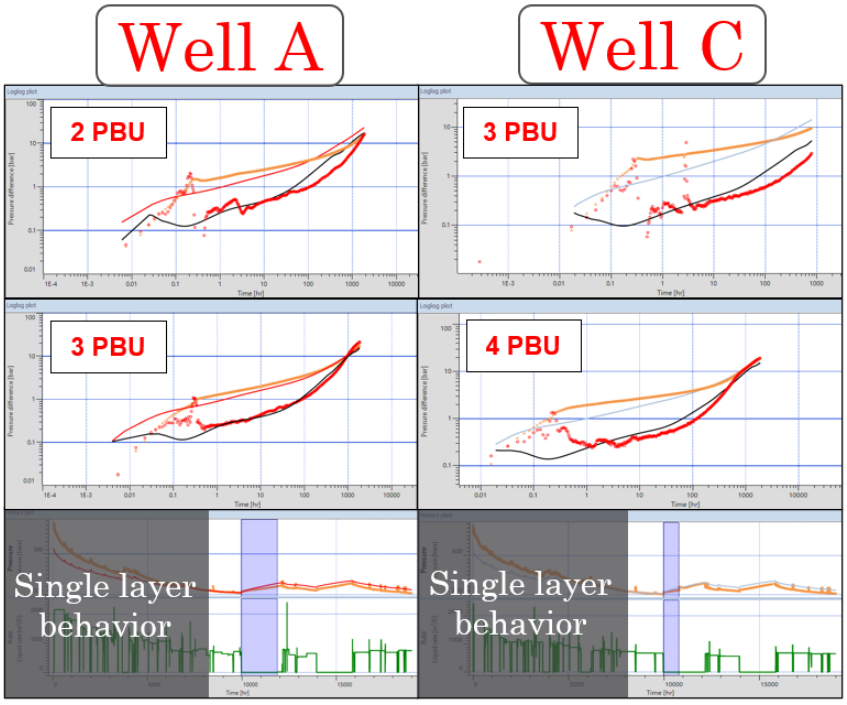

Figure 53. Multilayer model log-log plot and history plot after water injection started in the field for well A (left), and well C (right). Transmissibility between layers equal to 0.1.

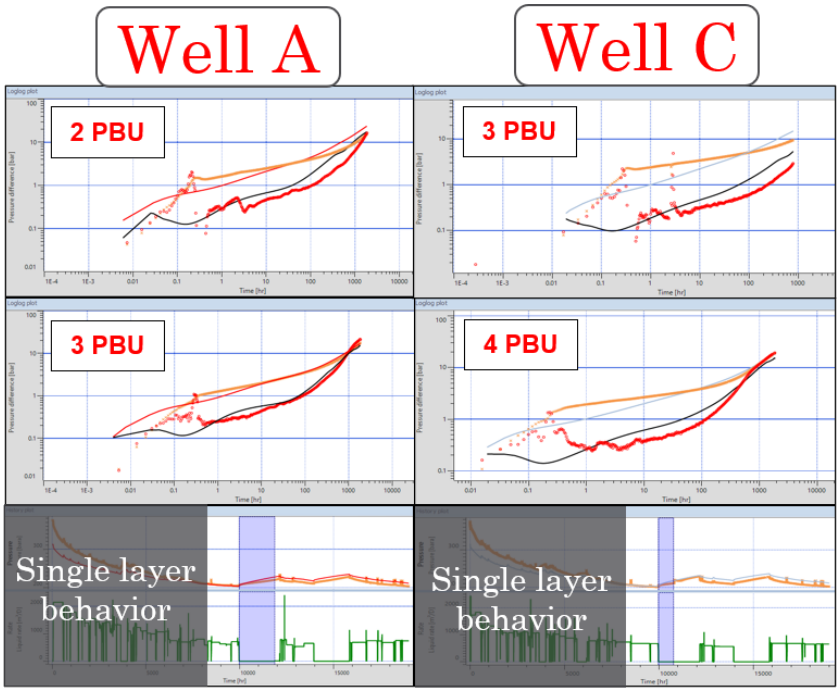

Figure 54. Multilayer model log-log plot and history plot after water injection started in the field for well A (left), and well C (right). Transmissibility between layers equal to 0.01.

7. Discussion and conclusions

The following conclusions may be drawn for comparison of analytical and numerical models:

- Analytical models may be capable of capturing the major well interference features as it was shown in this study.
- It was observed from pressure build-up (PBU) analysis of the horizontal wells using the analytical model, that it is possible to use the line-source well solution to approximate the nearby horizontal wells. The location for vertical well approximation of surrounding wells was selected close to the center of the horizontal section and showed good approximations as confirmed later with the numerical results.
- Numerical model allows to describe accurately complex reservoir flows and nonlinearities as it is important for long horizontal wells and complex reservoir geometries.
- Results from analytical models may be a good starting point for numerical simulations simplifying and accelerating history match of the numerical models.

The following conclusions may be done for time-lapse Pressure Transient Analysis (PTA) of the well data from the field. The wellbore storage effect masked the early-time cross-sectional radial flow for most of the PBUs and the late pseudo-radial flow period could not be observed due to the interference with the wells nearby or with the no-flow reservoir boundaries. Therefore, it's difficult to estimate kh from the pressure transients. However, some values of kh could be established for the reservoir describing the connected volumes in the history plot and matching the pressure derivatives, this for the wells A and C, parallel wells located at the south. The pressure response for well B showed a possible reduction in the kh values in the area around this well, confirmed with the numerical results.

Analysis of the interference of the production wells has revealed many interesting effects. Thus, in the interference analysis with time-lapse PBU interpretations, where well B is the observation well, and wells A and C are the active wells, it was shown that the pressure derivative going down at the late-time as a result of the continuous production of the surrounding wells as well as when these active wells are shut-in, but produced and depleted pressure in the area before. In this case, the same response in the pressure derivative is observed for the well B, when the active wells are shut-in (first PBU for well B) and the active wells are producing (second PBU for well B). This effect is related to the fact that well B started to produce after wells A and C depleted pressure in the region as it was confirmed by analytical and numerical simulations and history matching.

The time-lapse PTA revealed a characteristic change in the pressure derivative from the PBUs before and after water injection for well A and C. A shifting down of the derivatives after the injection well started to operate suggests an increase in the flow capacity of the reservoir or an increased effective well length. However, the increase in effective well length could not help to match the history using the numerical models. The multilayer model indicates that an increase in the thickness effectively contributing to the flow could be the

reason for such a change confirmed by history matching. The best match was achieved with a transmissibility value of 0.1 between the top and bottom layers.

The multi-well interference test, that considers the injection well as the active well and injecting water at the studied period and the three horizontal wells shut-in as the observation wells, confirms the reservoir communication between the producing wells and the injector. The time lag, that is the time required for the rate change at the active well to be observed at the observation wells, allows to characterize the reservoir parameters in the studied area. As discussed before, the results using the analytical and numerical models show a different kh value for the area around well B. The kh values that match the pressure response in the southern part for the first PBUs in well A and C, is high compared to the values observed in well B. The reduction in the injection rate that generates a pulse seen as a fluctuation in the pressure response in the well B occurs faster with the numerical model, an adequate match is obtained reducing the permeability from 80 mD to a value of 30 mD.

The observed time lag for the well B, the closest well to the injector, is 38 hr. approximately and similar to the match model that reduces the permeability (30 md) and thickness (10 m) with respect to the reference model. For well A, further than well B, the time lag is 54 hr. and a similar value to the simulated model that follows the reference model with a permeability of 80 md and a thickness of 12 m. For well C, the farthest producing well, the change is not observed in the derivative from the pressure response as it is seen in the model with the reservoir properties from the reference model with a time lag of about 154 hr.; this could indicate that the communication between the well C and the injector is not as good as the hydraulic connectivity of the reservoir between the well A and the injection well. Nonetheless, pressure support is provided to well C from the water injection as well.

To summarize, the following conclusions may be drawn from the analysis:

- The communication between produces was confirmed using analytical and numerical models.
- Pressure support from water injector to producers was verified using analytical and numerical models.
- The effects of increased or reduced effective well length from time-lapse PTA were studied and compared with the results with chemical PLT data. The effective well lengths provided by chemical PLT data are shorter than the drilled well lengths with a significant reduction for well A and C. However, according to PTA the effective well lengths could be larger than estimated from the chemical PLT. From time-lapse PTA, there is a change in the pressure derivative before and after injection for well A and C, indicating a possible increase in the effective well length after water injection starts. But this shift in the derivative was rather explained by an increase in pay thickness, since it provided better history match, than in case of the longer wells.
- Producing at bottom hole pressures below the bubble point did not present a strong effect.
- From time-lapse PTA, after water injection, there is an increase in kh suggested for wells A and C, as result of a possible contribution of bottom layer or inactive (during production) layers within the same geological unit.

- Area around well B has a lower kh than the other producing wells, also confirmed by interference with injector.
- Lower hydraulic connectivity between well C and the injection well than wells A and B and the injector was found.

8. Potential way forward

Time-lapse analysis of drawdown (DD) periods is an alternative approach (A. A. Shchipanov et al., 2014) to commonly used analysis of pressure buildups periods, that could provide further information of the reservoir is the focus. The pressure measurements from PDGs and flow rates allow to analyze long flowing transient periods, as shown in the figure below on the example of well A. Comparing the first DD observed in the well history with the first PBU (analyzed in the thesis), the longer DD period enables to cover a larger investigation area as it is shown in the figure below. As it may be seen from the log-log plot, a reduced productivity index may be interpreted for this DD if compared to the PBU (based on the pressure drop). Reasons may be well clean-up and increasing effective wellbore length.

The following advantages of analyzing transients from flowing periods may be highlighted:

- Ability to interpret live data from the beginning of production, without a need for shut-ins.
- Increased investigation radius due to longer durations of production periods compared to shut-ins.

At the same time, difficulties are also present, including noisy data due to rate fluctuations and need for testing of different rate averaging and derivative smoothing parameters. This analysis was out of the scope of the thesis, although preliminary tests confirmed potential for further testing and applying of this approach to the field data.

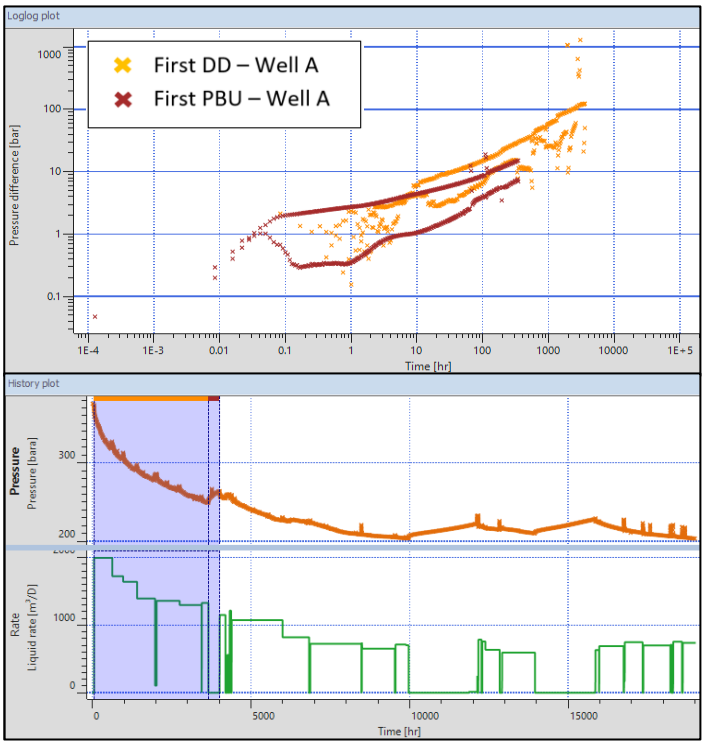

Figure 55. Pressure difference and derivative for DD and PBU periods (top) and history plot (bottom).

References

Akin, S. (2015). *Design and Analysis of Multiwell Interference Tests*. 10.

Al-Khamis, M. N., Ozkan, E., & Raghavan, R. S. (2005). Analysis of Interference Tests with Horizontal Wells. *SPE Reservoir Evaluation & Engineering*, *8*(04), 337–347. https://doi.org/10.2118/84292-PA

Al-Khamis, M., Ozkan, E., & Raghavan, R. (2001). Interference Testing with Horizontal Observation Wells. *SPE Annual Technical Conference and Exhibition*. SPE Annual Technical Conference and Exhibition, New Orleans, Louisiana. https://doi.org/10.2118/71581-MS

Awotunde, A. A., Al-Hashim, H. S., Al-Khamis, M. N., & Al-Yousef, H. Y. (2008). Interference Testing Using Finite-Conductivity Horizontal Wells of Unequal Lengths. *SPE Eastern Regional/AAPG Eastern Section Joint Meeting*. SPE Eastern Regional/AAPG Eastern Section Joint Meeting, Pittsburgh, Pennsylvania, USA. https://doi.org/10.2118/117744-MS

Bourdarot, G. (1998). *Well testing: Interpretation methods*. Editions Technip.

Bourdet, D. (2002). *Well test analysis: The use of advanced interpretation models* (1st ed). Elsevier.

Chaudhry, A. U. (2004). *Oil well testing handbook*. Gulf Professional Pub.

Elkins, L. F. (1946). Reservoir Performance and Well Spacing—Silica Arbuckle Pool, Kansas. *Oil & Gas J.*, 201–212.

Enyekwe, A. E., & Ajienka, J. A. (2014). Comparative Analysis of Permanent Downhole Gauges and their Applications. *SPE Nigeria Annual International*

Conference and Exhibition. SPE Nigeria Annual International Conference and Exhibition, Lagos, Nigeria. https://doi.org/10.2118/172435-MS

Gringarten, A. C., & London, I. C. (2008). *From Straight Lines to Deconvolution: The Evolution of the State of the Art in Well Test Analysis*. 22.

Halliburton. (2019). SmartFiber Pressure/Temperature Gauge. Retrieved from https://www.halliburton.com/content/dam/ps/public/pinnacle/contents/Data_Sheets/web/H013164-SmartFiber-Pressure-Temp-Gauge-SDS.pdf?node-id=ih3mevbr&nav=en-US_pinnacle_public

Houzé, O., & Viturat, D. (2020). *Dynamic Data Analysis*. 852.

Jacob, C. E. (1940). On the flow of water in an elastic artesian aquifer. *Transactions, American Geophysical Union*, *21*(2), 574. https://doi.org/10.1029/TR021i002p00574

Kamal, M. M. (1983). Interference and Pulse Testing-A Review. *Journal of Petroleum Technology*, *35*(12), 2257–2270. https://doi.org/10.2118/10042-PA

Kuchuk, F. J., Onur, M., & Hollaender, F. (2010). *Pressure transient formation and well testing: Convolution, deconvolution and nonlinear estimation* (1. ed). Elsevier.

Malekzadeh, D., & Tiab, D. (1991). Interference Testing of Horizontal Wells. *SPE Annual Technical Conference and Exhibition*. SPE Annual Technical Conference and Exhibition, Dallas, Texas. https://doi.org/10.2118/22733-MS

Nurafza, P. R., Al-Shamma, B., & Feng, W. C. (2014). Interference Testing of Horizontal Producers and Injectors in the Huntington Field. *International*

Petroleum Technology Conference. International Petroleum Technology Conference, Doha, Qatar. https://doi.org/10.2523/IPTC-17586-MS

Resman. (2018). Using Intelligent Tracer technology as an interventionless alternative to production logging. Retrieved from http://www.resman.no/site/wp-content/uploads/2018/02/RESMAN_Technical_Bulletin_1.Benefits.pdf

Sabet, M. A. (1991). *Well test analysis*. Gulf Pub. Co.

Schlumberger. (2018a). WellWatcher Sapphire. Retrieved from https://www.slb.com/-/media/files/co/product-sheet/sapphiregauge-ps.ashx

Schlumberger. (2018b). WellWatcher Quartz LT. Retrieved from https://www.slb.com/-/media/files/co/product-sheet/wellwatcher-quartz-lt-ps

Shchipanov, A., Kollbotn, L., & Berenblyum, R. (2017, June 12). *Integrating Pressure Transient Analysis into History Matching*. 79th EAGE Conference and Exhibition 2017, Paris, France. https://doi.org/10.3997/2214-4609.201700995

Shchipanov, Anton, Berenblyum, R., & Kollbotn, L. (2014). Pressure Transient Analysis as an Element of Permanent Reservoir Monitoring. *SPE Annual Technical Conference and Exhibition*. SPE Annual Technical Conference and Exhibition, Amsterdam, The Netherlands. https://doi.org/10.2118/170740-MS

Stewart, G. (2011). *Well test design & analysis*. PennWell.

Theis, C. V. (1935). The relation between the lowering of the Piezometric surface and the rate and duration of discharge of a well using ground-water storage.

Transactions, American Geophysical Union, *16*(2), 519. https://doi.org/10.1029/TR016i002p00519

Nomenclature

C	Wellbore storage coefficient, m^3/bar
Cr	Rock compressibility, bar^{-1}
Ct	Total compressibility, bar^{-1}
h	Formation thickness, m
k	Permeability, mD
k_h	Horizontal permeability, mD
kh	Reservoir flow capacity, mD-m
k_v	Vertical permeability, mD
k_v/k_h	Permeability anisotropy ratio, dimensionless
Lw	Well length, m
Pb	Bubble point pressure, bar
PBU	Pressure buildup
PDG	Pressure downhole gauge
Pi	Initial pressure, bar
PLT	Production logging tool
PTA	Pressure transient analysis
PV	Pore volume, m^3
S	Skin factor, dimensionless
μ	Fluid viscosity, cP
φ	Porosity, fraction

Appendix

- **Field production and injection data**

The combined history plot for all the studied wells, the horizontal producer and the deviated injection well is shown in figure below.

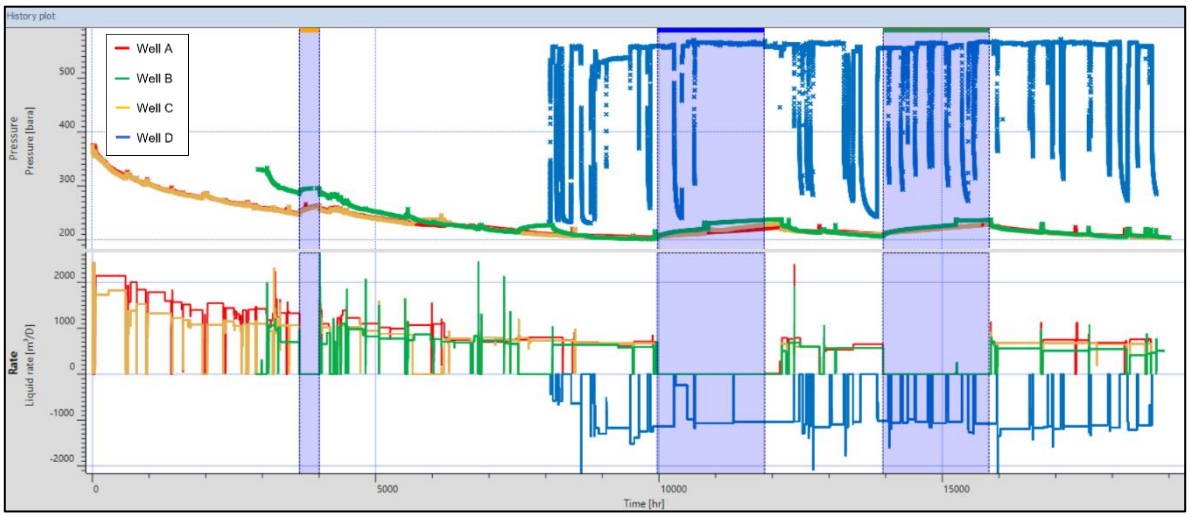

Figure 56. Combined history plot for all the production horizontal wells and the injection well. Pressure data at PDG, bara (top); and oil rate, m3/D (bottom) vs time, hr.